Universitat Autònoma de Barcelona
Facultat de Veterinària
Departament de Ciència Animal i dels Aliments

Validation of an optical technology to control the emulsification degree in meat emulsions

"Validación de una tecnología óptica de control del grado de emulsificación en emulsiones cárnicas''

Proyecto especial de graduación presentado para la superación de los 15 créditos del Módulo "Trabajo Fin de Máster" como requisito para optar al título de Máster en Calidad de Alimentos de Origen Animal

Presentado por

Erika Viviana Cabezas Tapia

Bellaterra, España
Julio, 2019

Directores:
Dra. Anna Zamora Viladomiu
Dra. Montserrat Mor-Mur Francesch
Dr. Manuel Castillo Zambudio

Declaro se la autora de este Trabajo Fin de Máster que se presenta para obtener el grado de Maestría en Calidad de Alimentos de Origen Animal en la Universidad Autònoma de Barcelona, España. Este trabajo no ha sido presentado antes para obtener ningún grado o examen en cualquier otra universidad.

Erika Viviana Cabezas Tapia
Bellaterra, 3 de julio de 2019

Los Drs. Anna Zamora Viladomiu, Manuel Castillo Zambudio y Montserrat Mor-Mur Francesch, investigadores del área de Tecnologia dels Aliments del Departament de Ciència Animal i dels Aliments de la Universitat Autònoma de Barcelona.

INFORMAN

Que el trabajo titulado: Validación de una tecnología óptica de control del grado de emulsificación en emulsiones cárnicas ha sido realizado, bajo su supervisión y tutela, por Erika Viviana Cabezas Tapia dentro del Máster en Calidad de Alimentos de Origen Animal de la Universitat Autònoma de Barcelona.

Bellatera, Julio de 2019

MANUEL CASTILLO ZAMBUDIO
Firmado digitalmente por MANUEL CASTILLO ZAMBUDIO
Nombre de reconocimiento (DN): c=ES, ou=Vegeu https://www.aoc.cat/CATCert/Regulacio, sn=CASTILLO ZAMBUDIO, givenName=MANUEL, serialNumber=27485164A, cn=MANUEL CASTILLO ZAMBUDIO
Fecha: 2019.07.03 13:27:01 +02'00'

Dr. Manuel Castillo Zambudio

ANNA ZAMORA VILADOMIU
Firmado digitalmente por ANNA ZAMORA VILADOMIU
Fecha: 2019.07.03 13:36:18 +02'00'

Dra. Anna Zamora Viladomiu

MONTSERRAT MOR-MUR FRANCESCH
Firmado digitalmente por MONTSERRAT MOR-MUR FRANCESCH
Nombre de reconocimiento (DN): c=ES, ou=Vegeu https://www.aoc.cat/CATCert/Regulacio, sn=MOR-MUR FRANCESCH, givenName=MONTSERRAT, serialNumber=40291939X, cn=MONTSERRAT MOR-MUR FRANCESCH
Fecha: 2019.07.03 13:34:12 +02'00'

Dra. Montserrat Mor-Mur

INDEX

ABSTRACT

The complex process of meat emulsions instability and the economic losses that can be generated, involves thinking about an improvement in the control of the emulsification process. Results from previous studies suggest that light-backscatter spectroscopy could provide information on emulsion stability. The purpose of this study was to validate a new multifiber optical sensor prototype able to detect inline the optimization degree of emulsification in meat emulsions. Batches produced at three chopping speeds (low, standard and high) were analyzed; this variability allowed differentiating quality parameters values (i.e., cooking losses, pH, moisture content, water activity and rheology of meat emulsions and texture of Frankfurters). 1610 optical parameters were obtained from the backscattered light spectra. Some optical predictors were found to correlate with quality parameters, of which some could be associated with elements of the chemical composition or quality of the meat matrix such us starch, fat, marbling and pigments. Finally, 12 basal predictors were used to predict the seven quality parameters through mathematical transformations (ratio, inverse, square and cube) using equations with the least number of predictors and with good statistical descriptors ($R^2 > 0.84$ and $CV < 5.00$).

Keywords: meat emulsion, cooking losses, quality parameters, optical predictors, light backscatter, correlations, prediction models, cross-validation.

RESUMEN

El complejo proceso de la inestabilidad de las emulsiones cárnicas, y las pérdidas económicas que con ello se pueden generar, conlleva a pensar en una mejora en el control del proceso de emulsificación. Los resultados de estudios previos sugieren que la espectroscopía de dispersión de luz podría proporcionar información sobre la estabilidad de la emulsión. El objetivo de este estudio fue validar un nuevo prototipo de sensor óptico multifibra capaz de detectar en línea el grado de optimización de la emulsión en emulsiones cárnicas. Se analizaron lotes producidos a tres velocidades de picado (baja, estándar y alta). Esta variabilidad debido a cambios en la velocidad permitió diferenciar los valores obtenidos para una serie de parámetros de calidad (pérdidas por cocción, pH, contenido de humedad, actividad de agua y reología de emulsiones cárnicas y textura de Frankfurts). De los espectros de luz dispersados, se obtuvieron 1610 parámetros ópticos. Algunos de los predictores ópticos mostraron correlaciones significativas ($P < 0.05$) con algunos de dichos parámetros, que podrían estar asociados con elementos de la composición química o de la calidad de la matriz cárnica, como el almidón, la grasa, el marmoleo y los pigmentos. Finalmente, se utilizaron 12 predictores basales para predecir los siete parámetros de calidad a través de transformaciones matemáticas (ratios, inversas, cuadrados y cubos) utilizando ecuaciones con el menor número de predictores y con buenos descriptores estadísticos (R2 > 0,84 y CV > 5.00).

Palabras clave: emulsión de carne, pérdidas por cocción, parámetros de calidad, predictores ópticos, dispersión de luz, correlaciones, modelos de predicción, validación cruzada.

1. INTRODUCTION

1.1. Meat and emulsions

Meat consumption is linked to factors such as: living standards, diet, livestock production, consumer prices, macroeconomic uncertainty, and Gross Domestic Product. Compared to other basic basket products, meat production generates high production costs and high output prices. In addition, the demand for meat is associated with higher incomes and with the interest of including in the diets the consumption of food that favors the increase of proteins of animal sources (OECD, 2018).

In general terms, an emulsion consists basically of two immiscible fluids one of which forms a dispersed phase within a continuous phase. Food emulsions are prepared from oil and water and depending on the emulsifier and the volume of oil-water, can be created as an oil-in-water (O/W) and water-in-oil (W/O) emulsions (Owusu-Apenten, 2004).

Meat emulsions consist of water, proteins, fat, salt and small amount of other ingredients. Products such as Frankfurters, Bologna, liver sausages and meat loaf are consumed all over the world and are of great economic importance to the meat industry. Emulsion meat products are produced from finely chopped or homogenized meat or mechanically recovered meat. The variables that can affect the characteristics of a meat emulsion are: chopping, temperature and intensity of emulsification, collagen content, fat melting point, ionic strength, meat postmortem physiology, proportion of fat, protein and water, salt soluble protein concentration and salt type (Owusu-Apenten, 2004).

Emulsion type sausage products are a stable mixture that binds water and traps and holds fat to form the characteristic texture of an emulsified product when it is cooked. The stability of this mixture depends, among other factors, on the extraction of salt-soluble meat proteins by the use of a bowl chopper or a combination of a mixer and an emulsifier (Knipe, 2014).

1.2. Meat emulsion stability

Food emulsions are defined as unstable systems and the increase in stability may be achieved by affecting phase separation kinetics and this stability can be extended by using effective emulsifiers, thickeners and stabilizers (Fredrick, Walstra, & Dewettinck, 2010).

Meat emulsion stability depends on water holding capacity or binding capacity of the meat proteins in the matrix. Salt increases the meat's ability to retain water during cooking, because

it adjusts the pH of the meat mixture to a point of greater water holding capacity and protein extraction. However, if a suitable combination of meat ingredients and appropriate processing procedures is performed (such as grinding, chopping and emulsifying), a stable emulsion will be obtained even during the cooking process. It is also important to understand the macroscopic behavior of the emulsion system with respect to the microstructural organization (Knipe, 2003).

As intrinsic and processing conditions affecting meat emulsions stability Zhu, Li, Li, Ning, & Zhou (2019) mention factors such as product composition, the quality of meat, physicochemical state of proteins, pH, food additives and ratio of fat/oil to protein.

Polysaccharides are good stabilizing agents due to their hydrophobicity and relatively high molecular weight. However, although improving processing stabilities and storage of meat emulsions, the addition of polysaccharides affects negatively rheological properties and quality of final products (Genccelep, Saricaoglu, Anil, Agar, & Turhan, 2015).

1.3. Economic impact

Finely comminuted meat products are an important part of diet in developed nations (USDA, 2017) and have great economic importance. According to data of USA for the year 2018, nearly 900 million pounds of hot dogs were sold at retail stores. That number represents that consumers spent more than $3 billion on hot dogs.

Experts believe sales of the entire refrigerated processed meat category will continue to grow in the future (NHDSC, 2016). Based on an average cooking loss of 2.64% in weight (optimum chopping conditions), the estimated economic losses by non-optimum emulsion stability range between 0.20 and 1.65 billion dollars per year depending on the production conditions. In Spain and Catalonia, it is estimated that the economic loss due to low stability ranges from 5 to over 40 million euros and 1 to 8 million euros, respectively.

1.4. Starch in meat emulsions

In a meat emulsion, fat globules are dispersed and stabilized in an aqueous matrix. Therefore, apart from the traditional ingredients used in the production of meat emulsions, starch, milk proteins, vegetable proteins, gums, fiber, and other surfactants are usually added since they act like binding agents within the emulsion (García-García & Totosaus, 2008).

Starch is a primary carbohydrate reserve present in plant tissues, and due to its low cost and wide availability, it is used in food and nonfood products to bestow various properties. Additionally to its nutritive value, it can be used to modify the physical properties of many foods. Commercial starches are mainly obtained from wheat, rice, corn, and tubers like potato, sweet potato, and cassava, which are commonly used in thickening, gelling, adhesion, stabilizing, moisture retention and texturizing applications (Balestra & Petracci, 2019). Specifically, it remains the dominant hydrocolloid used in food systems whether in modified or native forms and it is used in noodle, bakery, sauces, soups, dairy products, and meat products (Hong, Cheng, Gan, Lee, & Peh, 2018).

Starch is a common ingredient used to manufacture meat emulsions, by improving functional properties and stabilizing emulsion, enhancing viscosity or forming gels or as water binder to reduce formulation costs (Vasquez, de Francisco, & Bohrer, 2019). Starches are known to significantly increase yields, reduce cooking losses, increase moisture retention, improve texture and extend shelf life of meat products, for example the Frankfurters (González-Pérez & Arellano, 2009).

The most important criterion in choosing a starch for meat products is its gelatinization temperature that must correspond with the temperatures achieved during thermal processing of the meat product and close to the temperature at which the meat proteins denature and release water, so that the starch can be used to swell and hold moisture (Joly & Anderstein, 2009).

1.5. Backscatter technology

Few works have studied emulsion stability control using an optical sensor technology based in light backscatter; all these studies have demonstrated the relation between cooking losses and main quality parameters with the optical response and determined that light backscatter spectroscopy could provide information about emulsion stability (Álvarez, Castillo, Payne, Cox, & Xiong, 2009; Álvarez, Castillo, Payne, & Xiong, 2009; Álvarez, Castillo, Xiong, & Payne, 2010; Nieto, Xiong, Payne, & Castillo, 2014, 2015). The implementation of this type of control technology could contribute adjusting emulsification end-point, avoiding cooking losses and determining optimal quality parameters. Álvarez et al. (2009, 2010) studied the behavior of normalized light backscatter response, pH, color and cooking losses as a function of fat/lean ratio, chopping time, wavelength and fiber optic separation distance using different models. Their results suggest a high correlation between functional properties of meat

emulsion (i.e., fat/lean proportion) and specific peaks of the spectral scan. This means that light backscatter intensity of spectral scans, measured as normalized intensity on specific peaks, was inversely proportional to the different variables.

Previous studies carried out by our research group aimed at developing prediction models from optical data obtained from industrial samples with single-fiber optical sensors (Torres, 2016; González, 2017; Gibert, 2018). First, Torres (2016) found correlations between optical predictors (intensity and wavelength of peaks and slopes and their ratios) together with color and quality parameters in meat emulsions and Frankfurters (rheology and texture) with two different meat emulsion formulas (with and without starch). Then, the study of González (2017) focused on cooking losses instead of quality parameters and proposed models for predicting cooking losses using greater number of optical predictors (intensity and wavelength of peaks and slopes and their ratios, as the former study, plus some mathematical transformations) for meat emulsions with and without starch. Finally, Gibert (2018) used the actual values of slopes instead of wavelengths and intensities together with their ratios and mathematical transformations and found correlations between optical predictors and parameters such as cooking losses, rheology of emulsions and texture of Frankfurters, and proposed different prediction models for each of the parameters. It is necessary to mention that in her study, starch not only affected cooking losses and quality parameters but also interfered in the optical response of meat emulsions making more difficult to detect variations in the optical parameter caused by chopping speed and to stablish prediction models for emulsions with starch.

Thus, the objective of this study was to validate a new multifiber optical sensor prototype specifically designed by our research group and never studied to date, able to detect inline the degree of emulsification in meat emulsions with starch, which could be used as a tool to optimize both the cooking performance and the quality of both meat emulsions and Frankfurters.

2. MATERIALS AND METHODS

2.1. Sample preparation and characterization

Meat emulsions were produced by Grupo Alimentario ARGAL (Miralcamp, Spain), where lean meat, fat, salt, spices and other ingredients were mixed with an INOTEC industrial mixer (Model IM-4500, Reutlingen, Germany) to obtain a pre-chopped batter. Then, this batter was introduced into an INOTEC mill homogenizer (Model I175CDVM-90D), where the emulsification process occurred; three different speeds of homogenization were selected, set by changing the screw speed of the homogenizer and controlled through the outlet temperature of meat emulsions (i.e., 10, 7 and 5 ºC corresponding to low, standard and high-speed samples, respectively). About 1.5 kg of each type of emulsion was packed under vacuum and sent to Universitat Autònoma de Barcelona (UAB). In parallel, homogenized meat emulsions were stuffed in an edible collagen casing intended for human consumption to produce fresh, cured, cooked and/or smoked sausages. Cooked Frankfurters, about 15 cm long and 2 cm diameter, were also delivered cold and under vacuum by Grupo Alimentario ARGAL. Basic composition of both meat emulsions and Frankfurters was analyzed at the company using a food-scanning NIR Meat Analyzer (DK-3400, Foss Hillerød, Denmark).

2.2. Meat emulsion analyses

2.2.1. Light backscatter measurement

The analysis was carried out with a Fiber Optic Spectrometer (Model HR4000, Ocean Optics, Inc., Dunedin, FL, USA) connected to a power box (Powerflex TTi, DUAL CPX200) that provides electricity to the halogen bulb that is in the head of the optical sensor. The light bounces off the sample (backscatter) and the 4 fibers pick up the light signal. The information of the 4 fibers enters to the optical Fiber Spectrophotometer and are integrated into a single light signal (sum of intensities). Then this system sends optical data from the spectrometer to the computer across a USB cable to capture the optical spectra using the OceanView® software (v1.6.7, Ocean Optics, INC.) where the "y" axis of the spectrum represents the intensity signal (bits) and "x" axis, the wavelength (nm). About 25 g of meat emulsion was transferred to a sample holder; the optical sensor was placed on top of the holder and pressed until the supports of the sensor touched the edge of the sample holder to make sure that the sapphire window of the sensor was in touch with the meat sample. Measurements were done at room temperature (21-25 ºC) with 4.00 A and an integration time of 40 ms. Seven independent measurements at room temperature were carried out for each meat emulsion.

Like the analysis performed by Gibert (2018), the present study used the same procedure to detect the maximum slopes (rate of light backscatter intensity increase/decrease) of spectrum curves. The 3rd derivative of the response curve was used to detect the wavelengths at which the maximum slopes were most frequently observed (Fig. 1). Twenty-three slope points were identified from 340 nm to 1020 nm. The slope values were calculated also from the intensity vs. wavelength response curve using 40 points symmetrically located around each selected slope point and corresponded to a rank of 15.17 nm. Some mathematical transformations were calculated, such as ratios, squares, cubes and inverses using the averages of the slopes' values obtained with the first derivative. That is to say, the calculations were made in blocks. First block contained primary data (slopes only); the second block contained mathematical transformation of the slopes (squares, cubes and inverses). Third block contained slopes and ratios only, and the fourth block included slopes and ratios with their respective mathematical transformations (squares, cubes and inverses, the later only for slopes). A total of 1610 optical predictors were obtained to be statistically analyzed.

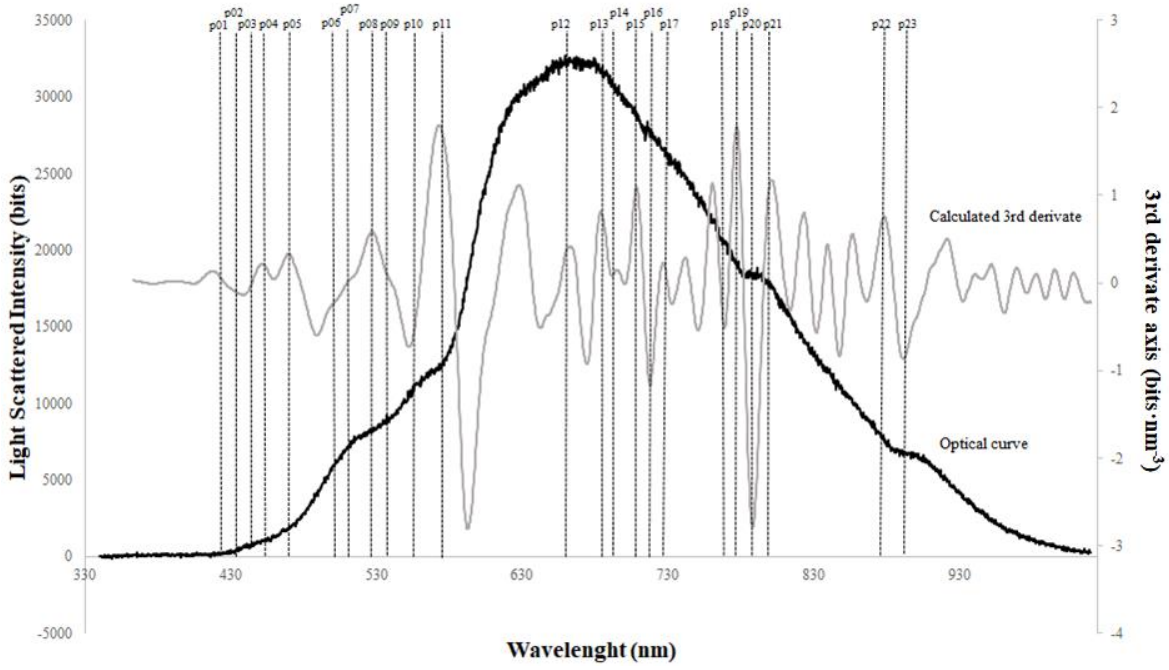

Fig. 1. Typical optical spectrum with the basal predictors

2.2.2. Cooking losses

For each type of meat sample, six tubes with 50 ml of meat emulsion were weighted and transferred to a preheated water bath at 75 ºC where the emulsions were cooked for 45 minutes. Tubes were removed from the bath and were placed inverted on a metal mesh during 1 min, to drain the expelled liquid. They were left to cool down at room temperature and finally were weighed. Cooking losses (CL) were calculated according to the equation:

$$\mathrm{CL}(\%) = \frac{w1-w2}{w1} x100 \quad \text{Eqn.1}$$

Where:
w1: Meat emulsion weight before cooking.
w2: Meat emulsion weight after cooking.

2.2.3. pH

The pH was determined in triplicate at room temperature in a meat slurry (10 g of meat emulsion : 10 g of distilled water) with a pH-meter (Basic 20, Crison, Barcelona, Spain).

2.2.4. Moisture content

Moisture content was determined through the Gravimetric method by ISO (1997). This evaluates the weight loss of the sample at 105 ºC for 24 h to constant weight, thus ensuring that all the moisture of the sample is volatilized and calculated according to the equation:

$$\text{Moisture } (\%) = \frac{w2-w3}{w2-w1} x100 \quad \text{Eqn.2}$$

Where:
w1: Weight of the capsule.
w2: Weight of the capsule plus wet sample.
w3: Weight of the capsule plus dry sample.

2.2.5. Water activity

Water activity (Aw) was determined in triplicate by the reference technique of water activity meters a_w AquaLab (Series 3 TE, Decagon Devices, In., Pullmann, Washington, USA) with the sensor technology of dew point. Disposable sample cups were filled with an amount that only covered the bottom of the sample cup. Since the temperature set in the AquaLab sampling chamber where the measurement is carried out is 25 °C, samples should be

temperate at about this temperature. The results were obtained in less than 5 min and with a precision of ± 0.003.

2.2.6. Rheology

Meat emulsion analysis was carried out in quadruplicate with a rotational rheometer (Rheo stress 1, Haake, Thermo Electron Corporation, Karlsruhe, Germany), coupled to a thermostatic bath (Phoneix C25P, Haake, Thermo Electron Corporation). A MPC/DC60 flat serrated plate and a PP60 top flat toothed probe were used and the zero point was calibrated. Meat emulsion samples were cautiously transferred from the pouch to the flat toothed base and slowly lowered the probe downward over the sample to a distance of 1mm from the baseplate, and excess meat emulsion was carefully eliminated.

Dynamic oscillatory test was performed at 21 ºC with a frequency sweep range of 1-100 Hz at a maximum strain of 0.01%. The Rheowin software (Rheo stress 1, Haake, Thermo Electron Corporation, Karlsruhe, Germany) was used to calculate the storage (*G*'), loss (*G*") and complex (*G**) moduli. Values of *G** at 10 Hz were stored and analyzed.

2.3. Frankfurters analysis: Texture

Uniaxial compression tests were performed with a TA-XT2 texture Analyzer (State microsystem, Surrey, UK). Three Frankfurters were analyzed per-trial and each one was cut with a blade in five cylindrical pieces of 1.9 mm height. The 15 Frankfurter pieces were compressed to 85% of their original height using a compression cylinder probe of 50 mm diameter at a cross-speed of 2 mm s^{-1}. Fracture force and distance were obtained using a macro in the Exponent program (Stable micro System, Surrey, UK).

2.4. Statistical analysis

A total of fifteen different trials were carried out (5 productions * 3 speeds). Variance analyses (Multifactor ANOVA) were performed with Statgraphics® program using speed, production and their interaction as factors. The LSD test was used to compare sample data, and the evaluations were based on a significance level of $P < 0.05$. Pearson's correlation coefficients (r) between optical predictors and cooking losses were determined using averages.

Prediction models were established to predict each quality parameters using as data the averages of the different batches for the 1610 optical predictors, and the "maximum R^2" procedure of the Statistical Analysis System (SAS®). To obtain the prediction models a maximum of eight variables and four blocks were used (slopes; slopes and transformations; slopes and ratios; slopes and ratios, and their transformations). Best regression models for predicting quality parameters were selected following the criteria: $R^2 \geq 0.84$, $CV \leq 5.00$ (Malley et al., 2005) and prediction equations with the least number of variables, for each parameter, and were fit to the corresponding data block, to evaluate the goodness of fit with each individual observation.

Cross-validation was only performed on the best models; selection was made by ordering the predictors used in the best models of each block for all quality parameters from the most to the least frequently observed. Models using less frequent predictors were discarded. This allowed the most representative models containing the predictors with a higher frequency to be selected in all equations. Cross-validation was performed with the SAS® system REG procedure, where the predictors used in each representative model were introduced. The system took one sample out and validated calculating new coefficients for the data left. This procedure was performed for each equation independently. Finally, the MEANS procedure provided the statistical parameters of the model using the different validations obtained separately.

3. RESULTS

3.1. Effect of chopping speed on studied parameters and correlations

Basic composition of both meat emulsions and Frankfurters, analyzed at the company, was: 66.29 and 63.17% moisture, 12.49 and 13.40% protein, 11.13 and 12.91% fat, 1.88 and 1.96% salt, 1.52 and 1.17% sugar, 1.65 and 1.98% collagen, for emulsions and Frankfurters, respectively.

Varying the speed of homogenization clearly affected both cooking losses and pH (Table 1). For both parameters, the three speeds significantly differed ($P < 0.05$) from each other. Regarding cooking losses, the observed trend was to increase as speed increased (from 2.35 to 2.84%). On the other hand, pH showed the lowest value in "standard" speed samples. However, both moisture content and water activity did not significantly differ ($P \geq 0.05$). As can be observed in Table 1, G^* was significantly differentiated ($P < 0.05$) in low speed samples, and its trend was to decrease as speed increased.

Table 1: Effect of speed on the different quality parameters.

Speed	Low	Standard	High
Cooking losses (%)[1]	2.35 ± 0.64 [c]	2.65 ± 0.61 [b]	2.84 ± 0.83 [a]
pH[2]	6.30 ± 0.20 [a]	6.26 ± 0.14 [c]	6.28 ± 0.17 [b]
Moisture (%)[2]	64.61 ± 1.10	64.70 ± 1.17	64.90 ± 0.98
Aw (%)[3]	97.32 ± 0.32	97.33 ± 0.27	97.40 ± 0.39
G (kPa)*[3]	16.98 ± 3.84 [a]	16.30 ± 3.71 [b]	16.12 ± 3.34 [b]
Force 1 (N)[4]	140.97 ± 38.01 [a]	144.98 ± 46.41 [a]	124.94 ± 22.14 [b]
Distance 1 (mm)[4]	14.87 ± 0.92 [a]	15.03 ± 1.37 [a]	14.56 ± 0.93 [b]

Mean value ± s.d.; [1]n=90, [2]n=45, [3]n=60, [4]n=225; [a-c]: values without common superscripts were significantly different ($P < 0.05$); Aw: water activity, G^*: complex modulus; Textural parameters: fracture force and distance.

Regarding the texture analysis of Frankfurters, a large number of analyzed samples showed a unique peak of fracture (Fig. 2). Hence, texture parameters of the second peak were not analyzed. Frankfurters texture profile was significantly affected ($P < 0.05$) by the chopping speed (Table 1). Frankfurters chopped at high speed needed of less force (124.94 N) in order to break and at the same time showed less plasticity (14.56 mm) than the other samples.

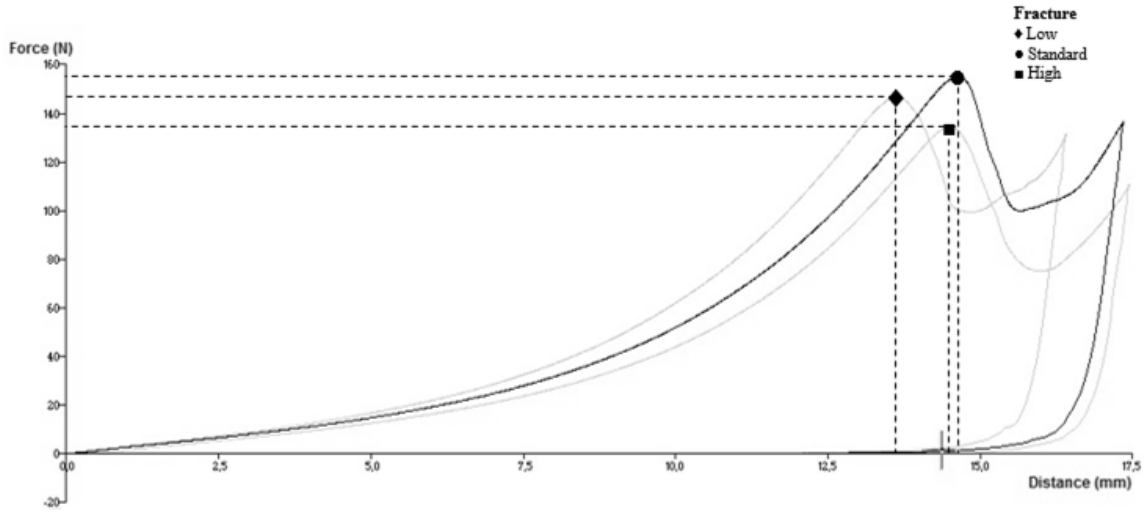

Fig. 2. Example of texture profile of one replicate of meat emulsion for each speed.

Concerning the optical response of meat emulsions depending on the chopping speed, none of the predictors was able to differentiate the three speeds. However, of the 23 basal predictors, eight (p06, p13, p14, p15, p16, p19, p21 and p22) differentiated at least one speed from the others (Table 2). Five (p02, p11, p17, p20 and p23) did not significantly differentiate ($P \geq 0.05$) between the three speeds. Furthermore, when taking the mathematical transformations, the inverse of p10 and the cube of p03 were not able to differentiate chopping speeds.

The eight predictors that differentiated at least one speed were distributed to the left and right sides of the maximum peak of optical spectra (675 nm). With the exception of p06 (517.66 nm), the rest of predictors were on the right side of the peak (from 688.792 to 879.19 nm). Regarding the five predictors that were not able to differentiate chopping speeds, they were evenly distributed in the optical spectra.

Due to the large quantity of ratios between slopes and their transformations, only ANOVA tests were performed for the "slopes ratios" values. The results showed that 276 predictors statistically differentiated ($P < 0.05$) one of the three processing speeds, and four predictors were able to statistically differentiate ($P < 0.05$) the three speeds (Table 3).

Table 2. Effect of chopping speed on the optical parameters of meat emulsions for slopes and their transformations.

Transf.	p			1/p		
Slopes	**Low**	**Std**	**High**	**Low**	**Std**	**High**
p01	25.82 ± 4.86 [a]	24.85 ± 3.85 [ab]	23.11 ± 6.20 [b]	0.04 ± 0.01 [b]	0.04 ± 0.01 [ab]	0.05 ± 0.01 [a]
p02	29.35 ± 6.02	27.32 ± 5.26	26.50 ± 4.26	0.04 ± 0.01	0.04 ± 0.01	0.04 ± 0.01
p03	37.43 ± 4.69 [a]	35.77 ± 5.97 [ab]	34.31 ± 6.95 [b]	0.03 ± 0.00 [b]	0.03 ± 0.00 [ab]	0.03 ± 0.01 [a]
p04	70.33 ± 12.94 [a]	67.06 ± 10.78 [ab]	63.53 ± 12.25 [b]	0.02 ± 0.00 [b]	0.02 ± 0.00 [ab]	0.02 ± 0.00 [a]
p05	142.41 ± 25.73 [a]	138.35 ± 20.21 [a]	128.97 ± 26.05 [b]	0.01 ± 0.00 [b]	0.01 ± 0.00 [b]	0.01 ± 0.00 [a]
p06	55.39 ± 17.18 [a]	54.99 ± 18.05 [a]	47.89 ± 15.49 [b]	0.02 ± 0.01 [b]	0.02 ± 0.01 [b]	0.02 ± 0.01 [a]
p07	47.11 ± 17.21 [a]	42.03 ± 20.62 [b]	38.38 ± 18.03 [b]	0.02 ± 0.01 [b]	0.03 ± 0.02 [ab]	0.03 ± 0.02 [a]
p08	79.20 ± 21.82 [a]	80.27 ± 21.98 [a]	71.07 ± 18.02 [b]	0.01 ± 0.00 [b]	0.01 ± 0.00 [b]	0.02 ± 0.00 [a]
p09	113.54 ± 21.64 [a]	110.32 ± 19.74 [a]	104.57 ± 19.35 [b]	0.01 ± 0.00 [b]	0.01 ± 0.00 [b]	0.01 ± 0.00 [a]
p10	125.17 ± 21.89 [a]	123.61 ± 20.59 [ab]	118.75 ± 15.94 [b]	0.01 ± 0.00	0.01 ± 0.00	0.01 ± 0.00
p11	506.23 ± 28.70	506.08 ± 29.90	500.41 ± 25.01	0.00 ± 0.00	0.00 ± 0.00	0.00 ± 0.00
p12	-27.73 ± 4.69 [a]	-26.28 ± 22.43 [a]	-37.52 ± 7.59 [b]	-0.04 ± 0.01 [ab]	-0.04 ± 0.00 [b]	-0.03 ± 0.01 [a]
p13	-97.82 ± 17.15 [a]	-102.18 ± 9.01 [a]	-125.79 ± 6.95 [b]	-0.01 ± 0.00 [b]	-0.01 ± 0.00 [b]	-0.01 ± 0.00 [a]
p14	-120.69 ± 12.54 [a]	-118.69 ± 13.41 [a]	-146.86 ± 5.05 [b]	-0.01 ± 0.00 [b]	-0.01 ± 0.00 [b]	-0.01 ± 0.00 [a]
p15	-152.04 ± 16.00 [a]	-153.74 ± 18.30 [a]	-179.34 ± 6.96 [b]	-0.01 ± 0.00 [b]	-0.01 ± 0.00 [b]	-0.01 ± 0.00 [a]
p16	-79.48 ± 8.03 [a]	-77.42 ± 9.65 [a]	-105.74 ± 12.64 [b]	-0.01 ± 0.00 [b]	-0.01 ± 0.00 [b]	-0.01 ± 0.00 [a]
p17	-117.20 ± 12.32	-117.63 ± 11.91	-119.25 ± 3.02	-0.01 ± 0.00	-0.01 ± 0.00	-0.01 ± 0.00
p18	-149.15 ± 15.51 [ab]	-150.57 ± 20.91 [b]	-140.10 ± 13.96 [a]	-0.01 ± 0.00 [a]	-0.01 ± 0.00 [a]	-0.01 ± 0.00 [b]
p19	-153.61 ± 18.15 [b]	-152.77 ± 16.43 [b]	-141.02 ± 20.29 [a]	-0.01 ± 0.00 [a]	-0.01 ± 0.00 [a]	-0.01 ± 0.00 [b]
p20	-9.04 ± 3.12	-9.21 ± 3.89	-9.80 ± 4.70	-0.13 ± 0.06	-0.12 ± 0.05	-0.17 ± 0.17
p21	-128.03 ± 14.38 [b]	-127.13 ± 14.13 [b]	-112.19 ± 16.62 [a]	-0.01 ± 0.00 [a]	-0.01 ± 0.00 [a]	-0.01 ± 0.00 [b]
p22	-108.55 ± 11.14 [b]	-106.41 ± 8.32 [b]	-92.19 ± 13.49 [a]	-0.01 ± 0.00 [a]	-0.01 ± 0.00 [a]	-0.01 ± 0.00 [b]
p23	-17.17 ± 2.75	-17.50 ± 2.99	-16.58 ± 3.65	-0.06 ± 0.01	-0.06 ± 0.01	-0.06 ± 0.02

Mean value ± s.d.; n=105; a-b: values per optical predictor without common superscripts were significantly different ($P < 0.05$); p: slope; 1/p: slope inverse.

Table 2. Effect of chopping speed on the optical parameters of meat emulsions for slopes and their transformations. (Continuation)

Transf.	p^2			p^3		
Slopes	**Low**	**Std**	**High**	**Low**	**Std**	**High**
p01	$6.85 \cdot 10^{2} \pm 2.70 \cdot 10^{2}$ a	$6.29 \cdot 10^{2} \pm 2.06 \cdot 10^{2}$ ab	$5.65 \cdot 10^{2} \pm 3.18 \cdot 10^{2}$ b	$1.87 \cdot 10^{4} \pm 1.14 \cdot 10^{4}$ a	$1.63 \cdot 10^{4} \pm 8.34 \cdot 10^{3}$ ab	$1.46 \cdot 10^{4} \pm 1.26 \cdot 10^{4}$ b
p02	$8.91 \cdot 10^{2} \pm 3.85 \cdot 10^{2}$	$7.69 \cdot 10^{2} \pm 3.10 \cdot 10^{2}$	$7.17 \cdot 10^{2} \pm 2.34 \cdot 10^{2}$	$2.80 \cdot 10^{4} \pm 1.89 \cdot 10^{4}$	$2.23 \cdot 10^{4} \pm 1.39 \cdot 10^{4}$	$1.98 \cdot 10^{4} \pm 9.78 \cdot 10^{3}$
p03	$1.42 \cdot 10^{3} \pm 3.62 \cdot 10^{2}$ a	$1.31 \cdot 10^{3} \pm 4.52 \cdot 10^{2}$ ab	$1.22 \cdot 10^{3} \pm 5.31 \cdot 10^{2}$ b	$5.45 \cdot 10^{4} \pm 2.12 \cdot 10^{4}$	$4.89 \cdot 10^{4} \pm 2.61 \cdot 10^{4}$	$4.47 \cdot 10^{4} \pm 3.09 \cdot 10^{4}$
p04	$5.08 \cdot 10^{3} \pm 1.98 \cdot 10^{3}$ a	$4.59 \cdot 10^{3} \pm 1.58 \cdot 10^{3}$ ab	$4.16 \cdot 10^{3} \pm 1.72 \cdot 10^{3}$ b	$3.78 \cdot 10^{5} \pm 2.31 \cdot 10^{5}$ a	$3.21 \cdot 10^{5} \pm 1.76 \cdot 10^{5}$ ab	$2.81 \cdot 10^{5} \pm 1.83 \cdot 10^{5}$ b
p05	$2.08 \cdot 10^{4} \pm 8.02 \cdot 10^{3}$ a	$1.95 \cdot 10^{4} \pm 6.02 \cdot 10^{3}$ a	$1.72 \cdot 10^{4} \pm 7.43 \cdot 10^{3}$ b	$3.13 \cdot 10^{6} \pm 1.90 \cdot 10^{6}$ a	$2.79 \cdot 10^{6} \pm 1.36 \cdot 10^{6}$ ab	$2.37 \cdot 10^{6} \pm 1.62 \cdot 10^{6}$ b
p06	$3.30 \cdot 10^{3} \pm 2.15 \cdot 10^{3}$ a	$3.28 \cdot 10^{3} \pm 2.29 \cdot 10^{3}$ a	$2.49 \cdot 10^{3} \pm 1.72 \cdot 10^{3}$ b	$2.12 \cdot 10^{5} \pm 2.11 \cdot 10^{5}$ a	$2.14 \cdot 10^{5} \pm 2.30 \cdot 10^{5}$ a	$1.40 \cdot 10^{5} \pm 1.49 \cdot 10^{5}$ b
p07	$2.46 \cdot 10^{3} \pm 1.77 \cdot 10^{3}$ a	$2.11 \cdot 10^{3} \pm 2.01 \cdot 10^{3}$ ab	$1.73 \cdot 10^{3} \pm 1.57 \cdot 10^{3}$ b	$1.40 \cdot 10^{5} \pm 1.47 \cdot 10^{5}$ a	$1.21 \cdot 10^{5} \pm 1.64 \cdot 10^{5}$ ab	$8.88 \cdot 10^{4} \pm 1.15 \cdot 10^{5}$ b
p08	$6.65 \cdot 10^{3} \pm 3.75 \cdot 10^{3}$ a	$6.83 \cdot 10^{3} \pm 4.00 \cdot 10^{3}$ a	$5.31 \cdot 10^{3} \pm 2.86 \cdot 10^{3}$ b	$5.92 \cdot 10^{5} \pm 5.04 \cdot 10^{5}$ ab	$6.18 \cdot 10^{5} \pm 5.65 \cdot 10^{5}$ a	$4.18 \cdot 10^{5} \pm 3.50 \cdot 10^{5}$ b
p09	$1.33 \cdot 10^{4} \pm 5.32 \cdot 10^{3}$ a	$1.25 \cdot 10^{4} \pm 4.61 \cdot 10^{3}$ ab	$1.12 \cdot 10^{4} \pm 4.39 \cdot 10^{3}$ b	$1.60 \cdot 10^{6} \pm 1.00 \cdot 10^{6}$ a	$1.45 \cdot 10^{6} \pm 8.21 \cdot 10^{5}$ ab	$1.24 \cdot 10^{6} \pm 7.60 \cdot 10^{5}$ b
p10	$1.61 \cdot 10^{4} \pm 5.82 \cdot 10^{3}$ a	$1.56 \cdot 10^{4} \pm 5.39 \cdot 10^{3}$ ab	$1.43 \cdot 10^{4} \pm 4.05 \cdot 10^{3}$ b	$2.11 \cdot 10^{6} \pm 1.19 \cdot 10^{6}$ a	$2.02 \cdot 10^{6} \pm 1.08 \cdot 10^{6}$ ab	$1.75 \cdot 10^{6} \pm 7.78 \cdot 10^{5}$ b
p11	$2.57 \cdot 10^{5} \pm 2.95 \cdot 10^{4}$	$2.57 \cdot 10^{5} \pm 3.05 \cdot 10^{4}$	$2.51 \cdot 10^{5} \pm 2.57 \cdot 10^{4}$	$1.31 \cdot 10^{8} \pm 2.28 \cdot 10^{7}$	$1.31 \cdot 10^{8} \pm 2.34 \cdot 10^{7}$	$1.26 \cdot 10^{8} \pm 1.98 \cdot 10^{7}$
p12	$7.86 \cdot 10^{2} \pm 2.61 \cdot 10^{2}$ b	$6.95 \cdot 10^{2} \pm 1.30 \cdot 10^{2}$ b	$1.45 \cdot 10^{3} \pm 5.37 \cdot 10^{2}$ a	$-2.28 \cdot 10^{4} \pm 1.11 \cdot 10^{4}$ a	$-1.85 \cdot 10^{4} \pm 5.28 \cdot 10^{3}$ a	$-5.78 \cdot 10^{4} \pm 2.94 \cdot 10^{4}$ b
p13	$9.80 \cdot 10^{3} \pm 3.61 \cdot 10^{3}$ b	$1.05 \cdot 10^{4} \pm 1.94 \cdot 10^{3}$ b	$1.59 \cdot 10^{4} \pm 1.74 \cdot 10^{3}$ a	$-1.01 \cdot 10^{6} \pm 5.80 \cdot 10^{5}$ a	$-1.09 \cdot 10^{6} \pm 3.14 \cdot 10^{5}$ a	$-2.00 \cdot 10^{6} \pm 3.28 \cdot 10^{5}$ b
p14	$1.47 \cdot 10^{4} \pm 3.08 \cdot 10^{3}$ b	$1.42 \cdot 10^{4} \pm 3.28 \cdot 10^{3}$ b	$2.16 \cdot 10^{4} \pm 1.48 \cdot 10^{3}$ a	$-1.80 \cdot 10^{6} \pm 5.71 \cdot 10^{5}$ a	$-1.72 \cdot 10^{6} \pm 6.09 \cdot 10^{5}$ a	$-3.18 \cdot 10^{6} \pm 3.26 \cdot 10^{5}$ b
p15	$2.33 \cdot 10^{4} \pm 4.98 \cdot 10^{3}$ b	$2.39 \cdot 10^{4} \pm 5.84 \cdot 10^{3}$ b	$3.22 \cdot 10^{4} \pm 2.47 \cdot 10^{3}$ a	$-3.61 \cdot 10^{6} \pm 1.17 \cdot 10^{6}$ a	$-3.76.10^{6} \pm 1.41 \cdot 10^{6}$ a	$-5.79 \cdot 10^{6} \pm 6.57 \cdot 10^{5}$ b
p16	$6.37 \cdot 10^{3} \pm 1.33 \cdot 10^{3}$ b	$6.07 \cdot 10^{3} \pm 1.56 \cdot 10^{3}$ b	$1.13 \cdot 10^{4} \pm 2.56 \cdot 10^{3}$ a	$-5.15 \cdot 10^{5} \pm 1.67 \cdot 10^{5}$ a	$-4.82 \cdot 10^{5} \pm 1.92 \cdot 10^{5}$ a	$-1.22 \cdot 10^{6} \pm 3.93 \cdot 10^{5}$ b
p17	$1.39 \cdot 10^{4} \pm 2.92 \cdot 10^{3}$	$1.39 \cdot 10^{4} \pm 2.84 \cdot 10^{3}$	$1.42 \cdot 10^{4} \pm 7.32 \cdot 10^{2}$	$-1.65 \cdot 10^{6} \pm 5.24 \cdot 10^{5}$	$-1.67 \cdot 10^{6} \pm 5.11 \cdot 10^{5}$	$-1.70 \cdot 10^{6} \pm 1.30 \cdot 10^{5}$
p18	$2.24 \cdot 10^{4} \pm 4.73 \cdot 10^{3}$ ab	$2.30 \cdot 10^{4} \pm 6.64 \cdot 10^{3}$ a	$1.98 \cdot 10^{4} \pm 4.09 \cdot 10^{3}$ b	$-3.41 \cdot 10^{6} \pm 1.09 \cdot 10^{6}$ ab	$-3.58 \cdot 10^{6} \pm 1.60 \cdot 10^{6}$ b	$-2.82 \cdot 10^{6} \pm 9.01 \cdot 10^{5}$ a
p19	$2.39 \cdot 10^{4} \pm 5.63 \cdot 10^{3}$ a	$2.36 \cdot 10^{4} \pm 5.12 \cdot 10^{3}$ a	$2.02 \cdot 10^{4} \pm 6.12 \cdot 10^{3}$ b	$-3.75 \cdot 10^{6} \pm 1.33 \cdot 10^{6}$ b	$-3.67 \cdot 10^{6} \pm 1.21 \cdot 10^{6}$ b	$-2.95 \cdot 10^{6} \pm 1.40 \cdot 10^{6}$ a
p20	$8.96 \cdot 10^{1} \pm 5.01 \cdot 10^{1}$	$9.69 \cdot 10^{1} \pm 7.82 \cdot 10^{1}$	$1.14 \cdot 10^{2} \pm 7.67 \cdot 10^{1}$	$-9.34 \cdot 10^{2} \pm 6.43 \cdot 10^{2}$	$-1.13 \cdot 10^{3} \pm 1.25 \cdot 10^{3}$	$-1.40 \cdot 10^{3} \pm 1.16 \cdot 10^{3}$
p21	$1.66 \cdot 10^{4} \pm 3.88 \cdot 10^{3}$ a	$1.63 \cdot 10^{4} \pm 3.78 \cdot 10^{3}$ a	$1.28 \cdot 10^{4} \pm 4.09 \cdot 10^{3}$ b	$-2.16 \cdot 10^{6} \pm 7.93 \cdot 10^{5}$ b	$-2.12 \cdot 10^{6} \pm 7.64 \cdot 10^{5}$ b	$-1.49 \cdot 10^{6} \pm 7.62 \cdot 10^{5}$ a
p22	$1.19 \cdot 10^{4} \pm 2.50 \cdot 10^{3}$ a	$1.14 \cdot 10^{4} \pm 1.82 \cdot 10^{3}$ a	$8.64 \cdot 10^{3} \pm 2.67 \cdot 10^{3}$ b	$-1.31 \cdot 10^{6} \pm 4.23 \cdot 10^{5}$ b	$-1.22 \cdot 10^{6} \pm 3.01 \cdot 10^{5}$ b	$-8.26 \cdot 10^{5} \pm 4.00 \cdot 10^{5}$ a
p23	$3.01 \cdot 10^{2} \pm 9.49 \cdot 10^{1}$	$3.13 \cdot 10^{2} \pm 1.03 \cdot 10^{2}$	$2.86 \cdot 10^{2} \pm 1.15 \cdot 10^{2}$	$-5.37 \cdot 10^{3} \pm 2.49 \cdot 10^{3}$	$-5.73 \cdot 10^{3} \pm 2.71 \cdot 10^{3}$	$-5.07 \cdot 10^{3} \pm 2.84 \cdot 10^{3}$

Mean value ± s.d.; n=105; a-b: values per optical predictor without common superscripts were significantly different ($P < 0.05$); p^2: slope square; p^3: slope cube.

Table 3. Ratios between slopes differentiating statistically chopping speed.

Ratios p																								
p01/p11	∙	p04/p16	∙	p07/p05	∙	p09/p13	∙	p11/p14	∙	p13/p05	∙	p14/p19	∙	p16/p06	∙	p17/p19	∙	p21/p10	∙
p01/p13	∙	p04/p17	∙	p07/p06	∙	p09/p14	∙	p11/p15	∙	p13/p06	∙	p14/p21	∙	p16/p07	∙	p17/p21	∙	p21/p11	∙
p01/p14	∙	p04/p21	∙	p07/p08	∙	p09/p15	∙	p11/p16	∙	p13/p07	∙	p14/p22	∙	p16/p08	∙	p17/p22	∙	p21/p12	∙
p01/p15	∙	p04/p22	∙	p07/p09	∙	p09/p16	∙	p11/p18	∙	p13/p08	∙	p14/p23	∙	p16/p09	∙	p18/p06	∙	p21/p13	∙
p01/p16	∙	p05/p11	∙	p07/p10	∙	p09/p17	∙	p11/p19	∙	p13/p09	∙	p15/p01	∙	p16/p10	∙	p18/p07	∙	p21/p14	∙
p01/p22	∙	p05/p12	∙	p07/p11	∙	p09/p21	∙	p11/p21	∙	p13/p10	∙	p15/p02	∙	p16/p11	∙	p18/p11	∙	p21/p15	∙
p02/p06	∙	p05/p13	∙	p07/p12	∙	p09/p22	∙	p11/p22	∙	p13/p11	∙	p15/p03	∙	p16/p15	∙	p18/p12	∙	p21/p16	∙
p02/p08	∙	p05/p14	∙	p07/p13	∙	p10/p06	∙	p12/p01	∙	p13/p15	∙	p15/p04	∙	p16/p17	∙	p18/p13	∙	p21/p17	∙
p02/p12	∙	p05/p15	∙	p07/p14	∙	p10/p07	∙	p12/p02	∙	p13/p17	∙	p15/p05	∙	p16/p18	∙	p18/p14	∙	p21/p18	∙
p02/p13	∙	p05/p16	∙	p07/p15	**X**	p10/p08	∙	p12/p03	∙	p13/p18	∙	p15/p06	∙	p16/p19	∙	p18/p15	∙	p21/p19	∙
p02/p14	∙	p05/p17	∙	p07/p16	∙	p10/p12	∙	p12/p04	∙	p13/p19	∙	p15/p07	∙	p16/p21	∙	p18/p16	∙	p22/p01	∙
p02/p15	∙	p05/p21	∙	p07/p17	∙	p10/p13	∙	p12/p05	∙	p13/p21	∙	p15/p08	∙	p16/p22	∙	p18/p17	∙	p22/p02	∙
p02/p16	∙	p05/p22	∙	p07/p18	∙	p10/p14	∙	p12/p06	∙	p13/p22	∙	p15/p09	∙	p16/p23	∙	p18/p21	∙	p22/p03	∙
p02/p17	∙	p06/p02	∙	p07/p19	∙	p10/p15	∙	p12/p07	∙	p13/p23	∙	p15/p10	∙	p17/p01	∙	p18/p22	∙	p22/p04	∙
p02/p22	∙	p06/p04	∙	p07/p21	∙	p10/p16	∙	p12/p08	∙	p14/p01	∙	p15/p11	∙	p17/p02	∙	p19/p11	∙	p22/p05	∙
p03/p11	∙	p06/p07	∙	p08/p02	∙	p10/p17	∙	p12/p09	∙	p14/p02	∙	p15/p13	∙	p17/p04	∙	p19/p12	∙	p22/p09	∙
p03/p13	∙	p06/p09	∙	p08/p09	∙	p10/p21	∙	p12/p10	∙	p14/p03	∙	p15/p14	∙	p17/p05	∙	p19/p13	∙	p22/p10	∙
p03/p14	∙	p06/p10	∙	p08/p10	∙	p10/p22	∙	p12/p11	∙	p14/p04	∙	p15/p16	∙	p17/p06	∙	p19/p14	∙	p22/p11	∙
p03/p15	∙	p06/p11	∙	p08/p11	∙	p11/p01	∙	p12/p17	∙	p14/p05	∙	p15/p17	∙	p17/p07	∙	p19/p15	∙	p22/p12	∙
p03/p16	∙	p06/p12	∙	p08/p12	∙	p11/p03	∙	p12/p18	∙	p14/p06	∙	p15/p18	∙	p17/p08	∙	p19/p16	∙	p22/p13	∙
p03/p21	∙	p06/p13	∙	p08/p13	∙	p11/p04	**X**	p12/p19	∙	p14/p07	∙	p15/p19	∙	p17/p09	∙	p19/p17	∙	p22/p14	∙
p03/p22	∙	p06/p14	∙	p08/p14	∙	p11/p05	∙	p12/p21	∙	p14/p08	∙	p15/p21	∙	p17/p10	∙	p19/p21	∙	p22/p15	∙
p04/p06	∙	p06/p15	∙	p08/p15	∙	p11/p06	∙	p12/p22	∙	p14/p09	∙	p15/p22	∙	p17/p12	∙	p19/p22	∙	p22/p16	∙
p04/p11	**X**	p06/p16	∙	p08/p16	∙	p11/p07	∙	p12/p23	∙	p14/p10	∙	p16/p01	∙	p17/p13	∙	p21/p02	∙	p22/p17	∙
p04/p12	∙	p06/p17	∙	p08/p17	∙	p11/p08	∙	p13/p01	∙	p14/p11	∙	p16/p02	∙	p17/p14	∙	p21/p03	∙	p22/p18	∙
p04/p13	∙	p06/p18	∙	p09/p06	∙	p11/p09	∙	p13/p02	∙	p14/p15	∙	p16/p03	∙	p17/p15	∙	p21/p04	**X**	p23/p12	∙
p04/p14	∙	p07/p03	∙	p09/p11	∙	p11/p12	∙	p13/p03	∙	p14/p17	∙	p16/p04	∙	p17/p16	∙	p21/p05	∙	p23/p13	∙
p04/p15	∙	p07/p04	∙	p09/p12	∙	p11/p13	∙	p13/p04	∙	p14/p18	∙	p16/p05	∙	p17/p18	∙	p21/p09	∙	p23/p14	∙

n=15 ∙: values of optical predictors with significant differences ($P < 0.05$) between one speed and the others; **x**: values of optical predictors with significant differences ($P < 0.05$) between the three speeds.

Considering Pearson's correlations between optical predictors and cooking losses (Table 4), sixteen of the predictors, both in their "slopes" and "square" form, fourteen in their "inverse" form and eighteen in their "cubic" form, presented a significant correlation ($P < 0.05$). Specifically, two of them (p09 and p19 which corresponded to 554 and 777 nm, respectively) were found to strongly correlate ($P \leq 0.001$) with cooking losses with absolute r values of 0.78-0.84 and 0.78-0.80, respectively. Other predictors such as p20 and p23 that started with a null significance ($P \geq 0.05$) and through mathematical transformations ended up having significant correlations ($P < 0.05$). On the contrary, although showing significant correlations ($P < 0.05$) as "slopes only", two predictors (p01 and p08 corresponding to 435 and 542 nm, respectively) lost significance when mathematically transformed. It should be noted that five predictors (p12, p13, p14, p15 and p16) had no correlation; these predictors were found within the optical spectrum in the zone between 675 and 718 nm (i.e., located immediately adjacent to the peak of the curve).

Table 4. Correlations between cooking losses and slopes and their transformations (inverse, square and cube) - Matrix with Pearson's coefficients.

Pred.	p	1/p	p^2	p^3
p01	-0.555 *	- ns	-0.570 *	-0.580 *
p02	-0.689 *	0.636 *	-0.637 *	-0.633 *
p03	-0.627 *	0.614 *	-0.628 *	-0.627 *
p04	-0.602 *	0.566 *	-0.613 *	-0.621 *
p05	-0.593 *	0.561 *	-0.604 *	-0.611 *
p06	-0.591 *	0.561 *	-0.599 *	-0.602 *
p07	-0.569 *	0.536 *	-0.579 *	-0.587 *
p08	-0.536 *	- ns	-0.555 *	-0.569 *
p09	-0.818 ***	0.843 ***	-0.800 ***	-0.780 ***
p10	-0.709 **	0.709 **	-0.704 **	-0.696 **
p11	-0.662 **	0.654 **	-0.666 **	-0.670 **
p12	- ns	- ns	- ns	- ns
p13	- ns	- ns	- ns	- ns
p14	- ns	- ns	- ns	- ns
p15	- ns	- ns	- ns	- ns
p16	- ns	- ns	- ns	- ns
p17	0.555 *	-0.525 *	-0.568 *	0.579 *
p18	0.643 **	-0.638 *	-0.641 **	0.637 *
p19	0.792 ***	-0.798 ***	-0.785 ***	0.777 ***
p20	- ns	- ns	- ns	0.522 *
p21	0.696 **	-0.674 **	-0.702 **	0.705 **
p22	0.627 *	-0.581 *	-0.646 **	0.661 **
p23	- ns	- ns	- ns	0.521 *

n=15; Significance: ns $P \geq 0.05$, * $P < 0.05$, ** $P \leq 0.01$, *** $P \leq 0.001$; Pred.: optical predictor; p: slope; 1/p: slope inverse; p^2: slope square; p^3: slope cube.

3.2. Prediction of quality parameters

3.2.1. Cooking losses

Using basal predictors, i.e., "slopes" block, it was already possible to obtain models to predict cooking losses with enough good statistical parameters and low number of variables (Table 5). The best model of this block used five variables and showed R^2, SEP and CV values of 0.98, 0.001 and 4.49, respectively.

Table 5. Statistical descriptors of the models for predicting cooking losses with optical predictors.

Cooking losses (%)				
	Number of variables	**R^2**	**SEP**	**CV**
Slopes	1	0.669	0.004	15.287
	2	0.887	0.002	9.301
	3	0.949	0.002	6.495
	4	0.971	0.001	5.143
	5	0.980	0.001	4.494
	6	0.988	0.001	3.666
	7	0.996	0.001	2.284
	8	0.997	0.001	2.178
Slopes and transformations	1	0.711	0.004	14.276
	2	0.910	0.002	8.281
	3	0.963	0.001	5.549
	4	0.977	0.001	4.589
	5	0.986	0.001	3.757
	6	0.994	0.001	2.667
	7	0.997	0.001	2.152
	8	0.998	0.000	1.810
Slopes and ratios	1	0.838	0.003	10.690
	2	0.896	0.002	8.907
	3	0.962	0.001	5.643
	4	0.983	0.001	3.924
	5	0.991	0.001	3.040
	6	0.995	0.001	2.310
	7	0.998	0.000	1.330
	8	0.999	0.000	0.468
Slopes, ratios and transformations	1	0.838	0.003	10.690
	2	0.896	0.002	8.907
	3	0.962	0.001	5.643
	4	0.983	0.001	3.924
	5	0.991	0.001	3.040
	6	0.995	0.001	2.310
	7	0.998	0.000	1.284
	8	0.999	0.000	0.468

n=15; R^2: determination coefficient; SEP: standard error of prediction; CV: coefficient of variation; Transformations: inverse, square and cube. Models in grey were the best models (R^2 > 0.84, CV < 5.00, together with lowest number of variables used).

Furthermore, for all the blocks, the best models (CV < 5.00) showed similar R^2 of 0.98. In other words, the inclusion of greater amount of data (i.e., ratios and transformations) slightly increased the coefficient of determination value (R^2) from 0.980 to 0.983 but with models using four variables instead of five. It should be noted that for the blocks "slopes and ratios" and "slopes, ratios and transformations", exactly the same statistical parameters were obtained since the same models were used for these two blocks. In other words, despite the inclusion of the mathematical transformations of slopes and ratios, the "maximum R^2" procedure did not select any of them as predictors.

3.2.2. pH, moisture and water activity of meat emulsions

Obtaining models for predicting pH, moisture and water activity of meat emulsions was also already possible with only basal predictors, i.e., "slope" block (Table 6). In the case of pH and water activity, increasing the amount of data (i.e., ratios and mathematical transformations) led to a decrease of the number of variables used in the best models from six down to four for pH and from five to three for water activity. R^2 increased from 0.85 to 0.96 and 0.90 to 0.92, for pH and water activity, respectively, and concomitant slight decreases of SEP and CV. However, in the case of moisture content of meat emulsions, for all four blocks, best models used only two variables with R^2 from 0.94 to 0.98. It should be also mentioned that for moisture and water activity, as for the case of cooking losses, the same models were found for "slopes and ratios" and "slopes, ratios and their transformations" blocks.

3.2.1. Rheology of meat emulsions and texture of Frankfurters

Complex modulus (G^*) only with the basal predictors ("slope" block) and its simple transformations ("slopes and transformations" block) obtained models using six and five variables, respectively, and with similar R^2, SEP and CV (Table 7). However, when ratios data was included, models with five variables showed slightly lower R^2 (0.974 vs. 0.990). Here again including the transformations of slopes and ratios did not alter the results.

As for the Frankfurters texture, it could be seen that the best prediction models of each block for the parameter fracture force obtained a R^2 of about 0.98 (Table 7). However, by increasing the amount of predictors (i.e., inclusion of slopes transformations, ratios and all transformations), the number of used variables in the equations of the models were lowered from six to three predictors. However, once again, the same models were obtained for the two blocks "slopes and ratios" and "slopes, ratios and their transformations".

Table 6. Statistical descriptors of the models for predicting pH, moisture and water activity parameters.

Parameters		pH			Moisture (%)			Water activity		
	Number of variables	R^2	SEP	CV	R^2	SEP	CV	R^2	SEP	CV
Slopes	1	0.306	0.136	2.166	0.888	0.004	0.543	0.188	0.005	0.487
	2	0.549	0.114	1.817	0.944	0.003	0.398	0.662	0.003	0.327
	3	0.624	0.109	1.734	0.983	0.001	0.229	0.735	0.003	0.302
	4	0.772	0.089	1.417	0.990	0.001	0.185	0.783	0.003	0.287
	5	0.822	0.083	1.319	0.994	0.001	0.150	0.896	0.002	0.209
	6	0.846	0.082	1.299	0.998	0.001	0.088	0.950	0.001	0.153
	7	0.880	0.077	1.227	0.999	0.001	0.080	0.962	0.001	0.144
	8	0.889	0.080	1.273	0.999	0.001	0.078	0.981	0.001	0.110
Slopes and transformations	1	0.338	0.133	2.116	0.903	0.003	0.505	0.276	0.004	0.428
	2	0.556	0.113	1.804	0.957	0.002	0.349	0.742	0.003	0.286
	3	0.787	0.082	1.304	0.975	0.002	0.277	0.823	0.002	0.247
	4	0.841	0.074	1.183	0.983	0.002	0.245	0.889	0.002	0.205
	5	0.956	0.041	0.655	0.987	0.001	0.224	0.930	0.002	0.173
	6	0.974	0.034	0.540	0.996	0.001	0.135	0.983	0.001	0.091
	7	0.982	0.030	0.478	0.997	0.001	0.114	0.992	0.001	0.068
	8	0.994	0.019	0.305	0.998	0.001	0.109	0.998	0.000	0.033
Slopes and ratios	1	0.466	0.119	1.901	0.920	0.003	0.458	0.656	0.003	0.317
	2	0.732	0.088	1.402	0.979	0.002	0.245	0.807	0.002	0.247
	3	0.846	0.070	1.108	0.993	0.001	0.145	0.915	0.002	0.171
	4	0.958	0.038	0.609	0.997	0.001	0.102	0.949	0.001	0.140
	5	0.976	0.030	0.484	0.998	0.001	0.078	0.974	0.001	0.104
	6	0.993	0.018	0.282	0.999	0.000	0.051	0.989	0.001	0.071
	7	0.998	0.010	0.154	1.000	0.000	0.015	0.999	0.000	0.017
	8	0.999	0.003	0.043	1.000	0.000	0.008	1.000	0.000	0.005
Slopes, ratios and transformations	1	0.466	0.119	1.901	0.920	0.003	0.458	0.656	0.003	0.317
	2	0.734	0.088	1.396	0.979	0.002	0.245	0.807	0.002	0.247
	3	0.847	0.070	1.107	0.993	0.001	0.145	0.915	0.002	0.171
	4	0.960	0.037	0.591	0.997	0.001	0.102	0.949	0.001	0.140
	5	0.976	0.030	0.485	0.998	0.001	0.078	0.974	0.001	0.104
	6	0.986	0.025	0.395	0.999	0.000	0.051	0.989	0.001	0.071
	7	0.994	0.017	0.274	1.000	0.000	0.015	0.999	0.000	0.017
	8	0.998	0.011	0.174	1.000	0.000	0.008	1.000	0.000	0.005

n=15; R^2: determination coefficient; SEP: standard error of prediction (units correspond to those of predicted parameters); CV: coefficient of variation (%); Transformations: inverse, square and cube. Models in grey were the best models ($R^2 > 0.84$, CV < 5.00, together with lowest number of variables used).

Table 7. Statistical descriptors of the models for predicting rheological and texture parameters.

	Parameters	*G* * (KPa)			Force (N)			Distance (mm)		
	Number of variables	R^2	SEP	CV	R^2	SEP	CV	R^2	SEP	CV
Slopes	1	0.642	2.234	13.567	0.369	30.212	22.059	0.306	0.817	5.513
	2	0.690	2.165	13.151	0.811	17.195	12.554	0.478	0.738	4.977
	3	0.842	1.614	9.800	0.939	10.197	7.445	0.694	0.590	3.978
	4	0.886	1.437	8.727	0.962	8.420	6.148	0.838	0.451	3.040
	5	0.957	0.927	5.633	0.976	7.098	5.182	0.886	0.397	2.680
	6	0.990	0.483	2.936	0.987	5.598	4.087	0.903	0.389	2.622
	7	0.992	0.456	2.769	0.990	5.129	3.745	0.913	0.394	2.656
	8	0.995	0.376	2.283	0.993	4.849	3.540	0.963	0.276	1.864
Slopes and transformations	1	0.720	1.976	11.999	0.373	30.130	21.999	0.410	0.753	5.082
	2	0.794	1.762	10.701	0.737	20.316	14.833	0.734	0.527	3.553
	3	0.889	1.350	8.199	0.939	10.197	7.445	0.849	0.415	2.799
	4	0.916	1.236	7.508	0.974	6.986	5.100	0.903	0.347	2.344
	5	0.990	0.451	2.740	0.986	5.483	4.003	0.952	0.258	1.742
	6	0.996	0.306	1.856	0.995	3.421	2.498	0.990	0.128	0.864
	7	0.997	0.271	1.648	0.998	2.482	1.812	0.994	0.108	0.729
	8	0.998	0.231	1.401	0.999	1.807	1.319	0.997	0.076	0.509
Slopes and ratios	1	0.740	1.905	11.572	0.787	17.546	12.811	0.438	0.735	4.958
	2	0.847	1.518	9.223	0.888	13.252	9.676	0.791	0.466	3.147
	3	0.914	1.190	7.229	0.983	5.377	3.926	0.952	0.233	1.569
	4	0.955	0.903	5.485	0.992	3.835	2.800	0.973	0.183	1.233
	5	0.974	0.727	4.413	0.996	2.805	2.048	0.989	0.122	0.825
	6	0.987	0.541	3.287	0.999	1.469	1.073	0.998	0.057	0.385
	7	0.998	0.251	1.525	0.999	1.124	0.821	0.999	0.028	0.187
	8	0.999	0.109	0.663	0.999	0.881	0.643	0.999	0.019	0.129
Slopes, ratios and transformations	1	0.740	1.905	11.572	0.787	17.546	12.811	0.438	0.735	4.958
	2	0.847	1.518	9.223	0.888	13.252	9.676	0.793	0.464	3.131
	3	0.914	1.190	7.229	0.983	5.377	3.926	0.955	0.226	1.525
	4	0.955	0.903	5.485	0.992	3.835	2.800	0.966	0.207	1.398
	5	0.974	0.727	4.413	0.996	2.805	2.048	0.985	0.146	0.983
	6	0.987	0.541	3.287	0.999	1.469	1.073	0.996	0.081	0.546
	7	0.998	0.251	1.525	0.999	1.093	0.798	0.999	0.029	0.199
	8	0.999	0.109	0.663	0.999	0.695	0.507	1.000	0.025	0.168

n=15; R^2: determination coefficient; SEP: standard error of prediction (units correspond to those of predicted parameters); CV: coefficient of variation (%); Transformations: inverse, square and cube. Models in grey were the best models ($R^2 > 0.84$, CV < 5.00, together with lowest number of predictors used).

Considering the prediction models of the textural parameter fracture distance, the inclusion of slopes transformations in the analysis resulted in a best model with a much lower number of variables (three vs. five) but with slightly lower R^2 (0.85 vs. 0.89) but similar SEP and CV (Table 7). When the ratios data was taken into consideration, best models also used three variables but got better statistical descriptors.

3.3. Summary of the best prediction models.

Table 8 summarizes the best selected models for each evaluated parameter with a $P \leq 0.001$ and an $R^2 > 0.84$. In the case of cooking losses, model IV of the "slopes and ratios" block with an R^2 of 0.983 was selected. This model used the mathematical forms p18/p09, $(p01/p06)^2$, $(p03/p05)^3$ and $(p03/p21)^3$. The fitting of predicted vs. experimental cooking losses showed that this model was very good to predict and explained the variability of the cooking losses (Figure 3). As can be seen in the graph the data of the experiment was adjusted to the linear model. R^2 having a value of 0.983 indicates that this model explained 98.30% of the variability observed in cooking losses. The cross-validation for this model showed an R^2 of 0.965 and CV of 3.927 %.

Model V of the "slopes and transformations" block, with basal predictors p20 and mathematical forms $(p03)^2$, $(p19)^2$, $(p03)^3$ and $(p21)^3$ was selected to predict the pH. The experimental data obtained were adjusted to the model obtaining a coefficient of determination R^2 of 0.956 (Figure 4a). The cross-validation for this model showed an R^2 of 0.905 and CV of 0.653 %. It should be noted that at first the model VI of the "slopes" block (in dark grey in table 9) was selected to predict the pH. However, when cross-validation was performed the R^2 was very low (R^2 of 0.546), so model was changed including more predictors.

For prediction of moisture content, selected model II of the "slopes only" block, with the basal predictors p06 and p20, showed an R^2 of 0.944, indicating that 94.4% of the experimental data fit to the linear model (Figure 4b). The cross-validation for this model showed an R^2 of 0.923 and CV of 0.399 %. Model III of the "slopes and ratios" block, with mathematical forms p09/p08, $(p22/p03)^2$ and $(p03/p22)^3$ was selected to predict the water activity. The fitting of predicted and experimental data showed an R^2 of 0.915 (Figure 4c). The cross-validation for this model obtained an R^2 of 0.865 and CV of 0.172 %.

Rheological parameter G^* was predicted with an R^2 of 0.974 using model V of the "slopes and ratios" block, with mathematical forms $(p20/p13)^2$, $(p05/p04)^3$, $(p11/p17)^3$, $(p20/p16)^3$ and $(p22/p09)^3$ (Figure 4d). The cross-validation for this model showed an R^2 of 0.917 and CV of 4.397 %. Considering the textural parameters, model VI of the "slopes" block, with the basal predictors p01, p03, p04, p05, p06 and p18 and model III of the "slopes and ratios", with the basal predictor p21 and mathematical forms $(p17/p15)^3$ and $(p20/p13)^3$, were selected to predict fracture force and distance, respectively. The fitting of the experimental

data allowed to obtain an R^2 of 0.987 and 0.952 for each textural parameter (Figure 4e and 4f). The cross-validation of the model for predicting fracture force resulted in an R^2 of 0.948 and CV of 4.038 %, and R^2 of 0.911 and CV of 1.569 % for fracture distance model.

Last but not least, it should be emphasized that only twelve basal predictors out of twenty-three (p01, p03, p04, p05, p06, p09, p13, p17, p18, p20, p21 and p22) were needed to predict the seven quality parameters.

Table 8. Summary table - Best prediction models of each quality parameter.

	Data	Models	Equations	R^2	SEP	CV
Cooking losses (%)	**a**	V***	$CL=0.016+0.001\ p_{01}+2.135\cdot10^{-4}\ p_{06}-8.809\cdot10^{-4}\ p_{09}+1.130\cdot10^{-4}\ p_{11}-7.563\cdot10^{-5}\ p_{12}$	0.980	0.001	4.494
	b	IV***	$CL=-0.034-1.141\ p_{530}+7.912\ p_{538}-2.789\ p_{551}+1.929\cdot10^{-5}\ p_{575}$	0.977	0.001	4.589
	c	IV***	$CL=-0.055-0.051\ p_{406}+0.071\ p_{580}-1.036\ p_{1152}-0.585\ p_{1168}$	0.983	0.001	3.924
	d	IV***	$CL=-0.055-0.051\ p_{406}+0.071\ p_{580}-1.036\ p_{1152}-0.585\ p_{1168}$	0.983	0.001	3.924
pH	**a**	VI**	$pH=5.693+0.004\ p_{11}+0.010\ p_{15}-0.015\ p_{17}-0.006\ p_{19}-0.030\ p_{20}+0.021\ p_{21}$	0.846	0.082	1.299
	b	V***	$pH=4.248-0.026\ p_{20}+0.004\ p_{555}+3.042\cdot10^{-5}\ p_{571}-6.178\cdot10^{-5}\ p_{1084}+2.854\cdot10^{-7}\ p_{1102}$	0.956	0.041	0.655
	c	IV***	$pH=9.323-0.006\ p_{11}+122.004\ p_{1008}-0.200\ p_{1426}+7.578\ p_{1528}$	0.958	0.038	0.609
	d	IV***	$pH=7.284+120.400\ p_{1008}-7.484\cdot10^{-9}\ p_{1092}-0.202\ p_{1426}+7.511\ p_{1528}$	0.960	0.037	0.591
Moisture (%)	**a**	II***	$M=0.674-6.430\cdot10^{-4}\ p_{06}-7.549\cdot10^{-4}\ p_{20}$	0.944	0.003	0.398
	b	II***	$M=0.694-3.176\ p_{538}-8.080\cdot10^{-6}\ p_{559}$	0.957	0.002	0.349
	c	II***	$M=0.665-0.042\ p_{445}-0.192\ p_{703}$	0.979	0.002	0.245
	d	II***	$M=0.665-0.042\ p_{445}-0.192\ p_{703}$	0.979	0.002	0.245
Water activity	**a**	V***	$Aw=0.977+0.002\ p_{01}+2.520\cdot10^{-4}\ p_{07}-7.827\cdot10^{-4}\ p_{08}-9.590\cdot10^{-4}\ p_{21}+0.001\ p_{22}$	0.896	0.002	0.209
	b	IV***	$Aw=0.964-1.905\ p_{535}+5.237\ p_{537}-6.829\cdot10^{-5}\ p_{555}+1.350\cdot10^{-6}\ p_{1084}$	0.889	0.002	0.205
	c	III***	$Aw=0.861+0.024\ p_{207}+0.005\ p_{1040}-0.865\ p_{1169}$	0.915	0.002	0.171
	d	III***	$Aw=0.861+0.024\ p_{207}+0.005\ p_{1040}-0.865\ p_{1169}$	0.915	0.002	0.171
G* **(KPa)**	**a**	VI***	$G^*=53.674-0.517\ p_{03}+0.699\ p_{04}-0.151\ p_{09}-0.112\ p_{10}-0.064\ p_{11}+0.340\ p_{20}$	0.990	0.483	2.936
	b	V***	$G^*=54.865+0.372\ p_{23}+6.586\cdot10^{2}\ p_{532}-2.334\cdot10^{3}\ p_{533}-4.970\cdot10^{-4}\ p_{571}-0.039\ p_{572}$	0.990	0.451	2.740
	c	V***	$G^*=32.341-7.244\cdot10^{2}\ p_{1006}-1.530\ p_{1196}+0.085\ p_{1340}+9.390\cdot10^{2}\ p_{1538}-9.647\ p_{1575}$	0.974	0.727	4.413
	d	V***	$G^*=32.341-7.244\cdot10^{2}\ p_{1006}-1.530\ p_{1196}+0.085\ p_{1340}+9.390.10^{2}\ p_{1538}-9.647\ p_{1575}$	0.974	0.727	4.413
Force (N)	**a**	VI***	$F=-746.110-4.168\ p_{01}-2.465\ p_{03}-3.077\ p_{04}+6.796\ p_{05}-13.972\ p_{06}-7.428\ p_{18}$	0.987	5.598	4.087
	b	V***	$F=-625.547+5.329\ p_{05}-12.971\ p_{06}-5.981\ p_{18}-11288\ p_{539}-0.004\ p_{1082}$	0.986	5.483	4.003
	c	III***	$F=-15.288+1.544\cdot10^{3}\ p_{1009}+40.404\ p_{1045}+7.929\cdot10^{2}\ p_{1063}$	0.983	5.377	3.926
	d	III***	$F=-15.288+1.544\cdot10^{3}\ p_{1009}+40.404\ p_{1045}+7.929\cdot10^{2}\ p_{1063}$	0.983	5.377	3.926
Distance (mm)	**a**	V***	$D=17.662-0.243\ p_{01}-0.061\ p_{14}+0.111\ p_{15}-0.096\ p_{17}-0.197\ p_{20}$	0.886	0.397	2.680
	b	III***	$D=33.161+0.153\ p_{23}+2.074\cdot10^{3}\ p_{547}-1.228\cdot10^{-5}\ p_{1088}$	0.849	0.415	2.799
	c	III***	$D=18.042+0.053\ p_{21}+6.083\ p_{1471}+8.852\cdot10^{2}\ p_{1535}$	0.952	0.233	1.569
	d	III***	$D=3.975-8.704\cdot10^{2}\ p_{550}+6.970\ p_{1471}+9.210\cdot10^{2}\ p_{1535}$	0.955	0.226	1.525

Data used: a: slopes only, b: slopes & transformations, c: slopes & ratios, d: all data. R^2: determination coefficient; SEP: standard error of prediction (units correspond to those of predicted parameters); CV: coefficient of variation (%). Models in light grey were the best models for each parameter (R2 > 0.84; CV < 5.00, and lowest number of predictors used), and were selected for cross-validation. Significance: *** $P \leq 0.001$. Model in dark gray was at first selected but showed a poor cross-validation.

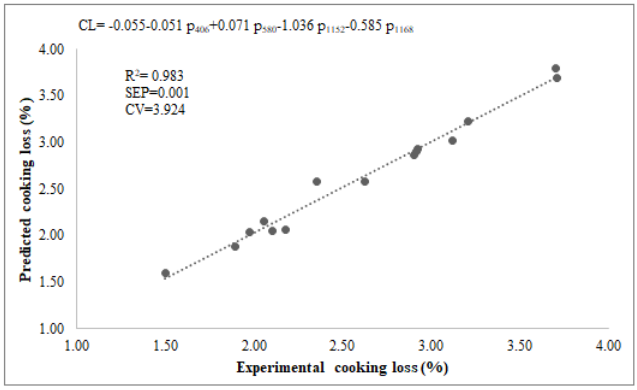

Fig. 3. Predicted values of cooking losses for meat emulsions obtained by Model IV ($P \leq 0.001$) with "slopes & ratios" data. R^2: determination coefficient; SEP: standard error of prediction (units correspond to those of predicted parameters); CV: coefficient of variation (%).

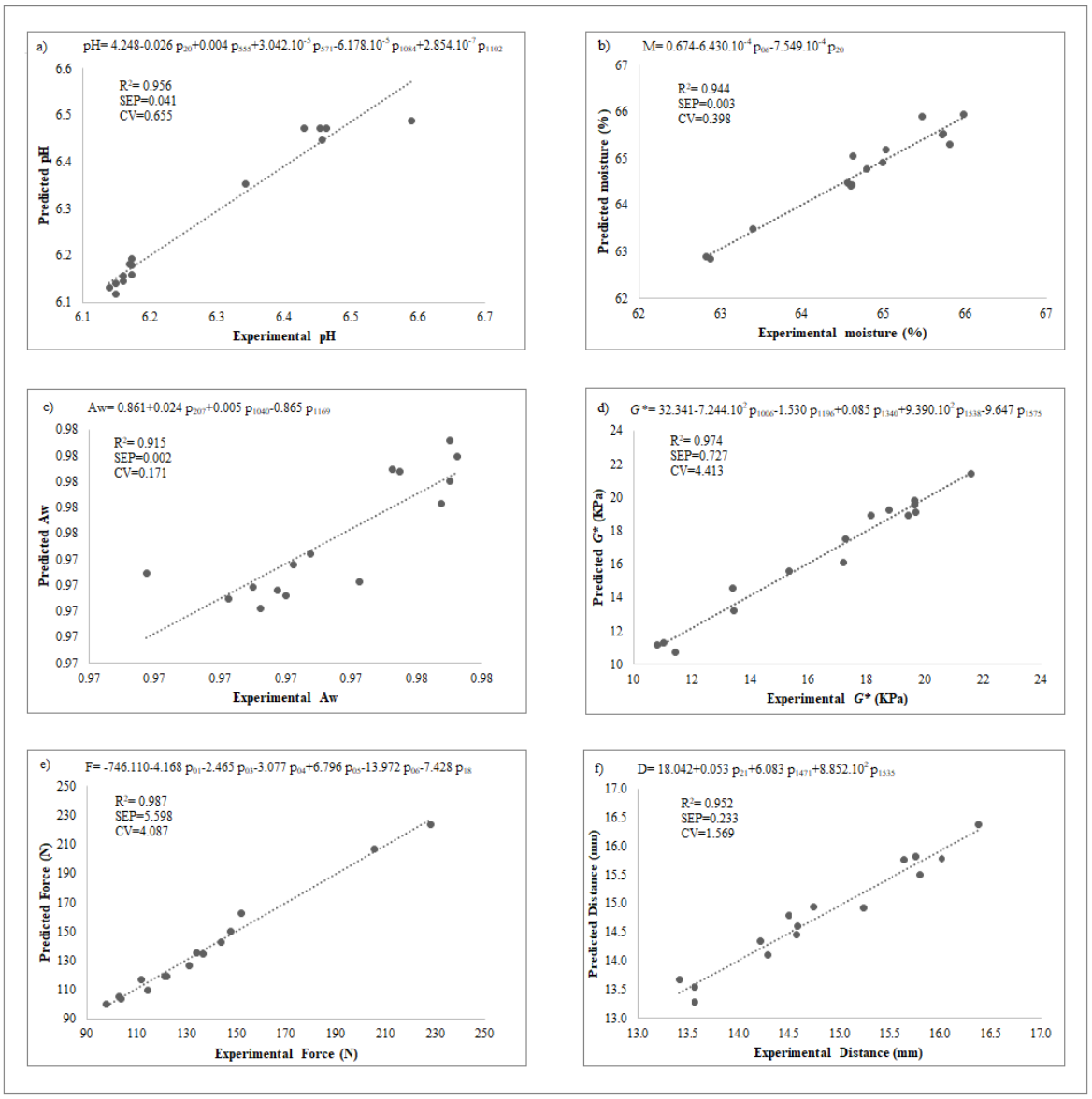

Fig. 4. Prediction models for quality parameters. a) Model Vb ($P \leq 0.001$) for pH, b) Model IIa ($P \leq 0.001$) for moisture, c) Model IIIc ($P \leq 0.001$) for water activity (Aw), d) Model Vc ($P \leq 0.001$) for complex modulus (G^*) of meat emulsions, e) Model VIa ($P \leq 0.001$) for textural parameter fracture force, f) Model IIIc ($P \leq 0.001$) for fracture distance of Frankfurters. R^2: determination coefficient; SEP: standard error of prediction (units correspond to those of predicted parameters); CV: coefficient of variation (%).

4. DISCUSSION

The variations due to the speed observed in this study allowed to differentiate the cooking losses, pH, rheology and texture. But parameters such as water activity and moisture were not differentiated. This is expected since meat emulsions had not yet undergone the cooking process. The factor that mainly affects water called free or unbound is protein modifications in relation to the change in three-dimensional structure since the water retention capacity is attributed to the myofibrillar proteins present in the meat (Adeyemi & Sazili, 2014). Taking into account that the objective of the present study was to find prediction models, the fact that changing chopping speed affected the studied parameter confirms that speeds were correctly selected.

Álvarez et al. (2007) found a positive correlation between cooking losses and increasing both chopping time and temperature in comminuted meat pork since over-chopping might result in softer gels. Similarly in the study of Allais, Viaud, Pierre, and Dufour (2004) with meat emulsions and Frankfurters, cooking losses increased when chopping time and speed increased from 3 to 7 minutes and from 2000 to 3000 rpm. In contrast, González (2017) and Gibert (2018) in their studies did not see a clear trend of the effect of speed on cooking losses. However, in the present study, it could be clearly seen a trend with cooking losses increasing from 2.35 to 2.84% as the speeds increased from low to high, with a middle value of 2.65% for standard speed.

The pH of pork fat and raw minced pork meat are usually in the range 6.67-7.71 and > 5.6, respectively (Paglarini et al., 2018; Del Blanco et al., 2017). In the present study, the pH average of all emulsions was 6.28 ± 0.15. pH values greatly depend on the formula of meat emulsions. At the industry level, pre-chopped batter is obtained by mixing lean meat, fat, salt, spices and other ingredients. It should be noticed that the results of the present study differ greatly with those obtained by Álvarez, Castillo, Payne, & Xiong (2009). They observed that depending on the chopping time, the pH can vary; in the first 5 min of chopping, pH increased significantly from 5.6 to 5.9 but after 8 min pH presented a slight decrease. The differences observed between these two studies can be explained by the chopping process itself. In the study of Álvarez et al. (2009), ingredients were comminuted in a bowl chopper (KitchenAid, Mod. KFP710, St. Joseph,Michigan, USA) at 1,750 rpm for 2, 5, and 8 min; instead, in the present study, comminuted meat emulsions were continuously produced at a rate of 7.000 kg/h with an industrial INOTEC mill homogenizer (Model I175CDVM-90D).

Rheological and textural properties are very important since these are related to many of the sensory attributes of emulsions. Rheology of meat emulsions and fracture of Frankfurters (i.e., force and distance) presented an inversely proportional relationship with speed. The viscoelastic parameter *G** decreased with the increase of chopping speed, which is in agreement with the results of Torres (2016) and Gibert (2018), where at a higher speed, lower was the overall strength of the emulsions to the deformation. The observed behavior of Frankfurters in terms of hardness was also in agreement with those obtained by Allais et al. (2004), Torres (2016) and Gibert (2018), where they found that the firmness of Frankfurters decreased as the chopping speed increased. The observed changes in rheological and textural properties could be explained by an inadequate emulsification process as the size of the fat particles can decrease greatly or changes at the emulsifying proteins of the meat, causing binding problems and soft gels (Barbut, 1998).

Variations in the optical response due to changes in the chopping speed observed in this study could be due to the fact that meat emulsions are complex compositional and structural materials. Differences in the basic components, i.e. water, proteins, fatty acids and/or lipids of meat products are the main factors that cause the deviation of a spectrum at a determined wavelength. On one hand, absorption/reflection behavior within the visible region of the spectra (380-780 nm) define color characteristics of the samples, which are affected by the chemical composition of the sample. Between 400 and 1100 nm (the wavelength range used in this study), light scatter properties originated by the interaction of light with the food particles becomes very relevant. On the other hand, food components have functional groups that contain certain chemical bonds (O-H, C-H, N-H, C-O, hydrogen bonds, etc.). Irradiation of IR light on these bonds results in vibrational responses that are recorded as a spectrum i.e. the bonds in the organic molecules of meat products absorb or emit infrared light when their vibratory state changes. Therefore, the biochemical components of a meat sample determine the amount and frequency of light absorbed, reflected or transmitted (Kumar & Chandrakant Karne, 2017).

Different optical parameters can be identified from the optical spectra. Gibert (2018) obtained approximately 444 predictors, distributed within the optical spectrum between 430 and 800 nm. However, a total of 1610 predictors distributed between 420 and 900 nm were obtained in the present study. Gibert (2018) obtained a greater number of predictors that differentiated at least one speed (with a few of them able to differentiate the three speeds)

and significantly correlated with cooking losses (i.e., with $r > 0.22$). In the present study, basal optical predictors only differentiated one chopping speed from the others, but as for Gibert (2018), some ratios were able to differentiate the three speeds. Furthermore, correlations with cooking losses were more significant than those of Gibert (2008) with $r > 0.55$). It can be said that having a greater number of predictors helped to get better information and much stronger correlations.

Beyond all the models obtained, the best prediction equations were found to predict all the quality parameters using only twelve basal predictors. The goodness of fit of these prediction equations was better than expected from a technological point of view, since in the meat industry R^2 of ~0.75 are good enough (INNOVAC, personal communication, October, 2017). Considering prediction of cooking losses, the best model proposed by González (2017) obtained a determination coefficient of $R^2 > 0.999$ for an equation with six variables, using data from the "peaks & slopes" block and their transformations. The best model proposed by Gibert (2018) obtained an $R^2 = 0.998$ for a model with five variables using all optical predictors (i.e., slopes and ratios, and their inverse, square and cube transformations). The determination coefficient of the present study was slightly lower ($R^2 = 0.983$) for a model with four variables. However, it should be emphasized that to obtain this model it was only necessary data from the "slopes & ratios" block. It should be noted in the study of Gibert (2018), none of the equations using "slopes only" data could be selected since none showed statistical descriptors above the required criteria.

On the contrary, in the present study, with only five of the basal predictors, it was already possible to obtain a good model ($R^2 = 0.980$) with the least number of variables, unlike the previous studies mentioned above. Regarding to models for the prediction of pH, moisture and water activity using only basal predictors, the determination coefficients were $R^2 > 0.84$, much higher than the technological threshold of 0.75. Including ratios and mathematical transformations increased R^2 to > 0.95 with models with fewer variables but with greater mathematical work and programming at the application level. The differences observed between previous studies and the present study showed that modifying the amount of fibers collecting the optical response of meat emulsions improved and simplified prediction models.

It should be noted that to predict textural parameters, Nieto et al. (2014) obtained an excellent prediction (R^2 of 0.99) for breaking force of the Frankfurters using an equation with five optical parameters using both light scatter and color parameters. Very similar results were

obtained in this study since the best model showed also excellent statistical parameters (R^2 = 0.987, CV = 4.087) with an equation with six variables and using only basal predictors.

In terms of wavelengths, the two strongest correlation values were found within the optical spectrum at points 554 and 776 nm and the five uncorrelated predictors were found in a range of 675 to 718 nm, i.e., the zone located immediately adjacent to the peak of the curve. These results differ from those obtained by Gibert (2018) with a single-fiber sensor, since she found three strong correlations ($r > 0.52$ and < 0.001) that were located at 470, 490 and 530 nm. Furthermore, no correlation of her predictors with the cooking losses were observed at 730 and 790 nm. Regarding to the most common basal predictors used in the best models to predict the parameters studied in both the present study and Gibert (2018), they were placed within the visible spectrum: twelve predictors (435, 459, 473, 493, 518, 554, 689, 729, 766, 788, 802 and 879 nm) against eight (490, 530, 550, 565, 590, 650, 675 and 730 nm) in Gibert (2018).

Since different components within a meat sample have particular absorption features, the nanometers information obtained may be associated with chemical composition and quality parameters. Cozzolino & Murray (2004) mentioned that in the visible region of the spectrum an absorption band at 430 nm was associated with the Soret absorption bond caused by traces of erythrocytes hemoglobin. Mamani-Linares, Gallo, & Alomar (2012) found that absorption bands at 560 and 595 nm were associated with pigments such us deoxy-myoglobin or oxymyoglobin. Furthermore, bearing in mind that meat emulsions had starch in their formulation, Barreto, Cruz-Tirado, Siche, & Quevedo (2018) found that the most important wavelength associated with the detection and prediction of starch in fresh cheese were at the wavelength of 584 nm. Qiao et al. (2007a, 2007b) selected six feature band images for predicting the drip loss (459, 618, 655, 685, 755 and 953 nm) and pH (494, 571, 637, 669, 703 and 978 nm) in pork meat and their study using hyperspectral imaging determined that marbling and lean in pork meat contrasted more at wavelengths between 580 and 720 nm, especially at 661 nm and water absorbing bands were observed at 750 and 950 nm. Finally, Mamani-Linares et al. (2012) mentioned that a band in the NIR region was observed at 990 nm and was related to fat. Some of the absorption bands mentioned were present in the models obtained in the present study, especially for cooking losses (e.g., p03 that corresponded to 459 nm).

5. CONCLUSION

The study on the response of new optical sensor prototype in meat emulsions with starch allowed for a clearer identification of information in areas of the spectrum curve that in previous studies showed a higher variability. Using the new prototype resulted in a stronger correlation between optical predictors and cooking losses and led to the development of prediction models with very good statistical parameters. In addition, 12 basal predictors were used to predict the seven quality parameters through mathematical transformations (ratio, inverse, square and cube) using equations with the least number of predictors and with good statistical descriptors. Finally, the obtained equations had the least number of optical predictors and, in some cases, did not include complicated mathematical transformations, an interesting point since it would ease the path for industrial transfer of the technology.

6. REFERENCES

Adeyemi, K. D., & Sazili, A. Q. (2014). Efficacy of carcass electrical stimulation in meat quality enhancement: a review. *Asian-Australasian Journal of Animal Sciences*, *27*(3), 447–456.

Allais, I., Viaud, C., Pierre, A., & Dufour, É. (2004). A rapid method based on front-face fluorescence spectroscopy for the monitoring of the texture of meat emulsions and frankfurters. *Meat Science*, *67*(2), 219–229.

Álvarez, D., Castillo, M., Payne, F. A., Cox, R. B., & Xiong, Y. L. (2009). Application of light extinction to determine stability of beef emulsions. *Journal of Food Engineering*, *96*, 309–315.

Álvarez, D., Castillo, M., Payne, F. A., Garrido, M. D., Bañón, S., & Xiong, Y. L. (2007). Prediction of meat emulsion stability using reflection photometry. *Journal of Food Engineering*, *82*(3), 310–315.

Álvarez, D., Castillo, M., Payne, F. A., & Xiong, Y. L. (2009). A novel fiber optic sensor to monitor beef meat emulsion stability using visible light scattering. *Meat Science*, *81*(3), 456–466.

Álvarez, D., Castillo, M., Xiong, Y. L., & Payne, F. A. (2010). Prediction of beef meat emulsion quality with apparent light backscatter extinction. *Food Research International*, *43*(5), 1260–1266.

Balestra, F., & Petracci, M. (2019). Technofunctional Ingredients for Meat Products. In C. Galanakis (Ed.). *Sustainable Meat Production and Processing* (pp. 45–68). Amsterdam-Netherlands: Academic Press.

Barbut, S., 1998. Use of a fiber optic probe to predict meat emulsion breakdown. *Italian Journal of Food Science*. 10,253-259

Barreto, A., Cruz-Tirado, J. P., Siche, R., & Quevedo, R. (2018). Determination of starch content in adulterated fresh cheese using hyperspectral imaging. *Food Bioscience*, *21*, 14–19.

Cozzolino, D., & Murray, I. (2004). Identification of animal meat muscles by visible and near infrared reflectance spectroscopy. *LWT - Food Science and Technology*, *37*(4), 447–452.

Del Blanco, A., Caro, I., Quinto, E. J., & Mateo, J. (2017). Quality changes in refrigerated stored minced pork wrapped with plastic cling film and the effect of glucose supplementation. *Meat Science*, *126*, 55–62.

Fredrick, E., Walstra, P., & Dewettinck, K. (2010). Factors governing partial coalescence in oil-in-water emulsions. *Advances in Colloid and Interface Science*, *153*(1–2), 30–42.

García-García, E., & Totosaus, A. (2008). Low-fat sodium-reduced sausages: Effect of the interaction between locust bean gum, potato starch and κ-carrageenan by a mixture design approach. *Meat Science*, *78*(4), 406–413.

Genccelep, H., Saricaoglu, F. T., Anil, M., Agar, B., & Turhan, S. (2015). The effect of starch modification and concentration on steady-state and dynamic rheology of meat emulsions. *Food Hydrocolloids*, *48*, 135–148.

Gibert, M. 2018. Optimization of meat emulsification using optical predictors (Master thesis). Universitat Autònoma de Barcelona, Spain.

González-Pérez, S., & Arellano, J. B. (2009). Vegetable protein isolates. In G.O. Philips & P.A. Williams (Ed) *Handbook of Hydrocolloids* (pp. 383–419). Sawston, Cambridge: Woodhead publishing

González, Z., 2017. Development of an optic control technology of the emulsification degree in meat emulsions (Master thesis). Universitat Autònoma de Barcelona, Spain.

Hong, L.-F., Cheng, L.-H., Gan, C.-Y., Lee, C. Y., & Peh, K. K. (2018). Evaluation of starch propionate as emulsion stabiliser in comparison with octenylsuccinate starch. *LWT*, *91*, 526–531.

ISO (1997). Determination of moisture content. ISO 1442:1997 Standard. In: International Standards Meat and Meat Products. International Organization for Standardization. Ginebra. Suiza.

Joly, G., & Anderstein, B. (2009). Starches. In R. Tarté (Ed.) *Ingredients in Meat Products* (pp. 25–55). Springer, New York, USA.

Knipe, C. L. (2014). Sausages, Types of | Emulsion. *Encyclopedia of Meat Sciences*, 256–260. Amsterdam-Netherlands: Academic Press.

Knipe, L. (2003). Emulsifiers | Phosphates as Meat Emulsion Stabilizers. *Encyclopedia of Food Sciences and Nutrition*, 2077–2080. Amsterdam-Netherlands: Academic Press

Kumar, Y., & Chandrakant Karne, S. (2017). Spectral analysis: A rapid tool for species detection in meat products. *Trends in Food Science & Technology*, *62*, 59–67.

Malley, D.F.; McClure, C.; Martin, P.D.; Buckley, K.; McCaughey, W.P. Compositional analysis of cattle manure during composting using a field-portable near-infrared spectrometer. *Commun. Soil Sci. Plant Anal.* **2005**, *36*, 455-475.

Mamani-Linares, L. W., Gallo, C., & Alomar, D. (2012). Identification of cattle, llama and horse meat by near infrared reflectance or transflectance spectroscopy. *Meat Science*,

90(2), 378–385.

NHDSC (National Hog Dog and sausage council) (2016). Vital hot dogs statistics. Recovered on June 7, 2019, of https://www.hot-dog.org/media/consumption-stats

Nieto, G., Xiong, Y. L., Payne, F., & Castillo, M. (2014). Predicting frankfurters quality metrics using light backscatter. *Journal of Food Engineering*, *143*, 132–138.

Nieto, G., Xiong, Y. L., Payne, F., & Castillo, M. (2015). Light backscatter fiber optic sensor: A new tool for predicting the stability of pork emulsions containing antioxidative potato protein hydrolysate. *Meat Science*, *100*, 262–268.

OECD (2018). Meat consumption. Recovered on June 6, 2019, of https://data.oecd.org/agroutput/meat-consumption.htm#indicator-chart

Owusu-Apenten, R. K. (2004). Testing protein functionality. *Proteins in Food Processing*, 217–244.

Paglarini, C. de S., Furtado, G. de F., Biachi, J. P., Vidal, V. A. S., Martini, S., Forte, M. B. S., … Pollonio, M. A. R. (2018). Functional emulsion gels with potential application in meat products. *Journal of Food Engineering*, *222*, 29–37.

Qiao, J., Wang, N., Ngadi, M. O., Gunenc, A., Monroy, M., Gariépy, C., & Prasher, S. O. (2007a). Prediction of drip-loss, pH, and color for pork using a hyperspectral imaging technique. *Meat Science*, *76*(1), 1–8.

Qiao, Jun, Ngadi, M. O., Wang, N., Gariépy, C., & Prasher, S. O. (2007b). Pork quality and marbling level assessment using a hyperspectral imaging system. *Journal of Food Engineering*, *83*(1), 10–16

Torres, V., 2016. Desarrollo de una tecnología óptica de control del grado de emulsificación en emulsiones cárnicas (Master thesis). Universitat Autònoma de Barcelona, Spain.

USDA (United States Department of Agriculture) (2017). Meat animals' production, disposition and income annual summary. Recovered on June 7, 2019, of https://usda.library.cornell.edu/concern/publications/02870v85d

Vasquez, S. M., de Francisco, A., & Bohrer, B. M. (2019). Replacing starch in beef emulsion models with β-glucan, microcrystalline cellulose, or a combination of β-glucan and microcrystalline cellulose. *Meat Science*, *153*, 58–65.

Zhu, X., Li, L., Li, S., Ning, C., & Zhou, C. (2019). l–Arginine/l–lysine improves emulsion stability of chicken sausage by increasing electrostatic repulsion of emulsion droplet and decreasing the interfacial tension of soybean oil-water. *Food Hydrocolloids*, *89*, 492–502.

7. ANNEXES

Annex 1. Models for the prediction of cooking losses in meat emulsions using all the optical predictors (slopes and ratios, and their mathematical transformations: inverse, square and cube).

Model		R^2	SEP	CV
I* **	**CL=** $\beta_0+\beta_1 p_{1487}$	0.838	0.003	10.690
II* **	**CL=** $\beta_0+\beta_1 p_{1487}+\beta_2 p_{1360}$	0.896	0.002	8.907
III* **	**CL=** $\beta_0+\beta_1 p_{1487}+\beta_3 p_{28}+\beta_4 p_{131}$	0.962	0.001	5.643
IV* **	**CL=** $\beta_0+\beta_5 p_{406}+\beta_6 p_{580}+\beta_7 p_{1152}+\beta_8 p_{1168}$	0.983	0.001	3.924
V* **	**CL=** $\beta_0+\beta_1 p_{1487}+\beta_7 p_{1152}+\beta_8 p_{1168}+\beta_9 p_{1109}+\beta_{10} p_{1190}$	0.991	0.001	3.040
VI* **	**CL=** $\beta_0+\beta_7 p_{1152}+\beta_8 p_{1168}+\beta_9 p_{1109}+\beta_{10} p_{1190}+\beta_{11} p_{958}+\beta_{12} p_{1607}$	0.995	0.001	2.310
VII* **	**CL=** $\beta_0+\beta_7 p_{1152}+\beta_8 p_{1168}+\beta_9 p_{1109}+\beta_{11} p_{958}+\beta_{13} p_{1019}+\beta_{14} p_{1104}+\beta_{15} p_{1548}$	0.998	0.000	1.284
VIII* **	**CL=** $\beta_0+\beta_7 p_{1152}+\beta_8 p_{1168}+\beta_9 p_{1109}+\beta_{11} p_{958}+\beta_{15} p_{1548}+\beta_{16} p_{63}+\beta_{17} p_{67}+\beta_{18} p_{661}$	0.999	0.000	0.468

n=15; CL: cooking losses; I-VIII: number of variables from 1 to 8; β_0-β_{18}: regression coefficients; p: predictor; R^2: determination coefficient; SEP: standard error of prediction; CV: coefficient of variation; Significance: * $P < 0.05$, ** $P \leq 0.01$, *** $P \leq 0.001$.

Annex 2. Regression coefficients values for cooking losses.

	Models							
	I* **	**II*** **	**III*** **	**IV*** **	**V*** **	**VI*** **	**VII*** **	**VIII*** **
β_0	-0.002 ns	-0.010 *	-0.067 ***	-0.055 ***	0.005 ns	-0.005 ns	-0.122 ***	0.081 ***
β_1	-0.011 ***	-0.011***	-0.010 ***	-	-0.009 ***	-	-	-
β_2		0.028 *	-	-	-	-	-	-
β_3			0.054 **	-	-	-	-	-
β_4			-0.037 **	-	-	-	-	-
β_5				-0.051 ***	-	-	-	-
β_6				0.071 ***	-	-	-	-
β_7				-1.036 ***	-1.427 ***	-1.556 ***	-1.606 ***	-1.696 ***
β_8				-0.585 ***	-0.912 ***	-1.015 ***	-1.033 ***	-1.140 ***
β_9					0.098 ***	0.102 *	0.126 ***	0.120 ***
β_{10}					0.059 ***	0.071 **	-	-
β_{11}						0.018 ***	0.018 ***	0.016 ***
β_{12}						1.015 *	-	-
β_{13}							0.082 ***	-
β_{14}							0.000 ***	-
β_{15}							0.028 ***	0.005 ***
β_{16}								-0.061 ***
β_{17}								0.003 ***
β_{18}								-0.231 ***

n=15; β_0-β_{18}: regression coefficients; Significance: ns $P \geq 0.05$, * $P < 0.05$, ** $P \leq 0.01$, *** $P \leq 0.001$.

Annex 3. Models for the prediction of pH in meat emulsions using all the optical predictors (slopes and ratios and their inverse, square and cube transformations).

Model		R^2	SEP	CV
I**	$pH = \beta_0 + \beta_1 p_{1537}$	0.466	0.119	1.901
II***	$pH = \beta_0 + \beta_2 p_{1008} + \beta_3 p_{1092}$	0.734	0.088	1.396
III***	$pH = \beta_0 + \beta_2 p_{1008} + \beta_4 p_{563} + \beta_5 p_{1528}$	0.847	0.070	1.107
IV***	$pH = \beta_0 + \beta_2 p_{1008} + \beta_3 p_{1092} + \beta_5 p_{1528} + \beta_6 p_{1426}$	0.960	0.037	0.591
V***	$pH = \beta_0 + \beta_2 p_{1008} + \beta_3 p_{1092} + \beta_5 p_{1528} + \beta_6 p_{1426} + \beta_7 p_{1579}$	0.976	0.030	0.485
VI***	$pH = \beta_0 + \beta_2 p_{1008} + \beta_3 p_{1092} + \beta_5 p_{1528} + \beta_6 p_{1426} + \beta_8 p_{1005} + \beta_9 p_{1107}$	0.986	0.025	0.395
VII***	$pH = \beta_0 + \beta_2 p_{1008} + \beta_4 p_{563} + \beta_5 p_{1528} + \beta_6 p_{1426} + \beta_8 p_{1005} + \beta_9 p_{1107} + \beta_{10} p_{1604}$	0.994	0.017	0.274
VIII***	$pH = \beta_0 + \beta_2 p_{1008} + \beta_3 p_{1092} + \beta_5 p_{1528} + \beta_6 p_{1426} + \beta_8 p_{1005} + \beta_9 p_{1107} + \beta_{10} p_{1604} + \beta_{11} p_{1490}$	0.998	0.011	0.174

n=15; β_0-β_{11}: regression coefficients; p: predictor; R^2: determination coefficient; SEP: standard error of prediction; CV: coefficient of variation; Significance: * $P < 0.05$, ** $P \leq 0.01$, *** $P \leq 0.001$.

Annex 4. Regression coefficients values for pH.

	Models							
	I**	II***	III***	IV***	V***	VI***	VII***	VIII***
β_0	6.147***	6.627***	7.378***	7.284***	7.341***	7.643***	8.653 ***	9.180**
β_1	515.622 **	-	-	-	-	-	-	-
β_2		72.240***	115.540***	120.400 ***	132.278***	225.713***	300.963 ***	375.177 ***
β_3		-4.77.10-9 **	-	-7.48.10-9 **	-8.08.10-9 **	-9.02.10-9***	-	-1.11.10-8 ***
β_4			-5.71.10-6 **	-	-	-	-8.13.10-6 ***	-
β_5			6.903*	7.511 ***	9.535***	11.316***	12.090 ***	11.957***
β_6				-0.202 ***	-0.175***	-0.204***	-0.240 ***	-0.258***
β_7					-0.055*	-	-	-
β_8						-30.736 *	-56.703 **	-86.186***
β_9						-4.995 **	-8.090***	-10.714***
β_{10}							7.875 *	9.180**
β_{11}								0.025*

n=15; β_0-β_{11}: regression coefficients; Significance: ns $P \geq 0.05$, * $P < 0.05$, ** $P \leq 0.01$, *** $P \leq 0.001$.

Annex 5. Models for the prediction of moisture in meat emulsions using all the optical predictors (slopes and ratios and their inverse, square and cube transformations).

Model		R^2	SEP	CV
I* **	**M=** $\beta_0+\beta_1 p_{703}$	0.920	0.003	0.458
II* **	**M=** $\beta_0+\beta_1 p_{703}+\beta_2 p_{445}$	0.979	0.002	0.245
III* **	**M=** $\beta_0+\beta_3 p_{217}+\beta_4 p_{693}+\beta_5 p_{1004}$	0.993	0.001	0.145
IV* **	**M=** $\beta_0+\beta_4 p_{693}+\beta_5 p_{1004}+\beta_6 p_{428}+\beta_7 p_{1576}$	0.997	0.001	0.102
V* **	**M=** $\beta_0+\beta_4 p_{693}+\beta_5 p_{1004}+\beta_6 p_{428}+\beta_7 p_{1576}+\beta_8 p_{1562}$	0.998	0.001	0.078
VI* **	**M=** $\beta_0+\beta_4 p_{693}+\beta_5 p_{1004}+\beta_6 p_{428}+\beta_7 p_{1576}+\beta_8 p_{1562}+\beta_9 p_{08}$	0.999	0.000	0.051
VII* **	**M=** $\beta_0+\beta_4 p_{693}+\beta_5 p_{1004}+\beta_6 p_{428}+\beta_7 p_{1576}+\beta_9 p_{08}+\beta_{10} p_{1033}+\beta_{11} p_{1472}$	1.000	0.000	0.015
VIII* **	**M=** $\beta_0+\beta_4 p_{693}+\beta_5 p_{1004}+\beta_6 p_{428}+\beta_7 p_{1576}+\beta_9 p_{08}+\beta_{10} p_{1033}+\beta_{11} p_{1472}+\beta_{12} p_{1001}$	1.000	0.000	0.008

n=15; M: moisture; β_0-β_{12}: regression coefficients; p: predictor; R^2: determination coefficient; SEP: standard error of prediction; CV: coefficient of variation; Significance: * $P < 0.05$, ** $P \leq 0.01$, *** $P \leq 0.001$.

Annex 6. Regression coefficients values for moisture.

	Models							
	I* **	**II*** **	**III*** **	**IV*** **	**V*** **	**VI*** **	**VII*** **	**VIII*** **
β_0	0.672 ***	0.665 ***	0.758 ***	0.560 ***	0.573 ***	0.572 ***	0.593***	0.591***
β_1	-0.197 ***	-0.192 ***	-	-	-	-	-	-
β_2		-0.042 ***	-	-	-	-	-	-
β_3			0.131 ***	-	-	-	-	-
β_4			-0.095 ***	-0.093 ***	-0.094 ***	-0.129 ***	-0.144***	-0.142***
β_5			18.838***	20.371***	18.418***	16.618***	14.089 ***	15.866***
β_6				-0.072 ***	-0.065 ***	-0.066 ***	-0.060***	-0.061***
β_7				-0.004 **	-0.008 ***	-0.014 ***	-0.014***	-0.013***
β_8					-0.008 *	-0.021 ***	-	-
β_9						1.46.10-4 **	1.77.10-4 ***	1.58.10-4 ***
β_{10}							-0.034 ***	-0.032***
β_{11}							5.29.10-4 ***	5.07.10-4 ***
β_{12}								-0.023 ***

n=15; β_0-β_{12}: regression coefficients; Significance: ns $P \geq 0.05$ * $P < 0.05$, ** $P \leq 0.01$, *** $P \leq 0.001$.

Annex 7. Models for the prediction of Aw in meat emulsions using all the optical predictors (slopes and ratios and their inverse, square and cube transformations).

Model		R^2	SEP	CV
I* **	$A_w = \beta_0 + \beta_1 p_{185}$	0.656	0.003	0.317
II* **	$A_w = \beta_0 + \beta_2 p_{207} + \beta_3 p_{1169}$	0.807	0.002	0.247
III* **	$A_w = \beta_0 + \beta_2 p_{207} + \beta_3 p_{1169} + \beta_4 p_{1040}$	0.915	0.002	0.171
IV* **	$A_w = \beta_0 + \beta_1 p_{185} + \beta_3 p_{1169} + \beta_4 p_{1040} + \beta_5 p_{1453}$	0.949	0.001	0.14
V* **	$A_w = \beta_0 + \beta_1 p_{185} + \beta_3 p_{1169} + \beta_5 p_{1453} + \beta_6 p_{1569} + \beta_7 p_{1589}$	0.974	0.001	0.104
VI* **	$A_w = \beta_0 + \beta_1 p_{185} + \beta_3 p_{1169} + \beta_5 p_{1453} + \beta_7 p_{1589} + \beta_8 p_{488} + \beta_9 p_{1607}$	0.989	0.001	0.071
VII* **	$A_w = \beta_0 + \beta_3 p_{1169} + \beta_7 p_{1589} + \beta_{10} p_{640} + \beta_{11} p_{737} + \beta_{12} p_{1037} + \beta_{13} p_{1255} + \beta_{14} p_{1431}$	0.999	0.000	0.017
VIII* **	$A_w = \beta_0 + \beta_3 p_{1169} + \beta_7 p_{1589} + \beta_{11} p_{737} + \beta_{12} p_{1037} + \beta_{13} p_{1255} + \beta_{14} p_{1431} + \beta_{15} p_{88} + \beta_{16} p_{1592}$	1.000	0.000	0.005

n=15; Aw: water activity; β_0-β_{16}: regression coefficients; p: predictor; R^2: determination coefficient; SEP: standard error of prediction; CV: coefficient of variation; Significance: * $P < 0.05$, ** $P \leq 0.01$, *** $P \leq 0.001$.

Annex 8. Regression coefficients values for Aw.

	Models							
	I* **	**II*** **	**III*** **	**IV*** **	**V*** **	**VI*** **	**VII*** **	**VIII*** **
β_0	1.006 ***	0.936 ***	0.861 ***	0.945 ***	0.961 ***	0.881 ***	1.014 ***	1.057 ***
β_1	-0.046 ***	-	-	-0.054 ***	-0.050 ***	-0.046 ***	-	-
β_2		0.021 ***	0.024 ***	-	-	-	-	-
β_3		-0.186 **	-0.865 ***	-0.771 ***	-0.667 ***	-0.950 ***	-2.478 ***	-1.379 ***
β_4			0.005 **	0.004 **	-	-	-	-
β_5				-2.57.10-8 *	-5.77.10-8**	-8.78.10-8***	-	-
β_6					6.92.10-4 **	-	-	-
β_7					-0.007 *	-0.016 ***	-0.016 ***	-0.014 ***
β_8						-0.029 ***	-	-
β_9						-2.956 ***	-	-
β_{10}							-1.149 ***	-
β_{11}							-0.037 ***	-0.036 ***
β_{12}							9.33.10-5 ***	1.06.10-4 ***
β_{13}							-9.56.10-6 ***	-9.19.10-6 ***
β_{14}							-9.65.10-8 ***	-9.28.10-8 ***
β_{15}								0.396 ***
β_{16}								-0.085 ***

n=15; β_0-β_{16}: regression coefficients; Significance: ns $P \geq 0.05$ * $P < 0.05$, ** $P \leq 0.01$, *** $P \leq 0.001$.

Annex 9. Models for the prediction of *G** in meat emulsions using all the optical predictors (slopes and ratios and their inverse, square and cube transformations).

Model		R^2	SEP	CV
I***	$G^* = \beta_0+\beta_1 p_{1537}$	0.740	1.905	11.572
II***	$G^* = \beta_0+\beta_2 p_{220}+\beta_3 p_{1006}$	0.847	1.518	9.223
III***	$G^* = \beta_0+\beta_3 p_{1106}+\beta_4 p_{1046}+\beta_5 p_{1340}$	0.914	1.190	7.229
IV***	$G^* = \beta_0+\beta_3 p_{1106}+\beta_4 p_{1046}+\beta_5 p_{1340}+\beta_6 p_{1196}$	0.955	0.903	5.485
V***	$G^* = \beta_0+\beta_3 p_{1006}+\beta_5 p_{1340152}+\beta_6 p_{1196}+\beta_7 p_{1538}+\beta_8 p_{1575}$	0.974	0.727	4.413
VI***	$G^* = \beta_0+\beta_3 p_{1006}+\beta_5 p_{1340}+\beta_6 p_{1196}+\beta_8 p_{1575}+\beta_9 p_{1109}+\beta_{10} p_{1320}$	0.987	0.541	3.287
VII***	$G^* = \beta_0+\beta_3 p_{1006}+\beta_7 p_{1538}+\beta_8 p_{1575}+\beta_{10} p_{1320}+\beta_{11} p_{63}+\beta_{12} p_{811}+\beta_{13} p_{1174}$	0.998	0.251	1.525
VIII***	$G^* = \beta_0+\beta_3 p_{1006}+\beta_5 p_{1340}+\beta_7 p_{1538}+\beta_8 p_{1575}+\beta_{10} p_{1320}+\beta_{11} p_{63}+\beta_{14} p_{463+}\beta_{15} p_{645}$	0.999	0.109	0.663

n=15; *G**: complex modulus; β_0-β_{15}: regression coefficients; p: predictor; R^2: determination coefficient; SEP: standard error of prediction; CV: coefficient of variation; Significance: * $P < 0.05$, ** $P \leq 0.01$, *** $P \leq 0.001$

Annex 10. Regression coefficients values for *G**.

	Models							
	I***	**II*****	**III*****	**IV*****	**V*****	**VI*****	**VII*****	**VIII*****
β_0	20.233 ***	35.579 ***	14.294 ***	26.243 ***	32.341 ***	48.743 ***	13.651 ***	-1.074 ns
β_1	-14861 ***	-	-	-	-	-	-	-
β_2		14.259 **	-	-	-	-	-	-
β_3		-464.051 ***	-395.766 ***	-450.146 ***	-724.388 ***	-898.015 ***	-899.474 ***	-988.848 ***
β_4			13.170 ***	13.969 ***	-	-	-	-
β_5			0.080 *	0.085 **	0.085 ***	0.117 ***	-	0.112 ***
β_6				-1.392 *	-1.530 **	-2.285***	-	-
β_7					939.037 *	-	1155.548 ***	1338.919 ***
β_8					-9.647 ***	-7.900 ***	-6.344 ***	-6.493 ***
β_9						235.696 **	-	-
β_{10}						12.231 **	232.725 ***	22.926 ***
β_{11}							-63.115 ***	-61.408 ***
β_{12}							-0.779 ***	-
β_{13}							158.169 ***	-
β_{14}								1.121 ***
β_{15}								114.305 ***

n=15; β_0-β_{15}: regression coefficients; Significance: ns $P \geq 0.05$ * $P < 0.05$, ** $P \leq 0.01$, *** $P \leq 0.001$.

Annex 11. Models for the prediction of fracture force in Frankfurters using all the optical predictors (slopes and ratios and their inverse, square and cube transformations).

Model		R^2	SEP	CV
I* **	**F=** $\beta_0+\beta_1 p_{1574}$	0.787	17.546	12.811
II* **	**F=** $\beta_0+\beta_1 p_{1574}+\beta_2 p_{1593}$	0.888	13.252	9.676
III* **	**F=** $\beta_0+\beta_3 p_{1009}+\beta_4 p_{1045}+\beta_5 p_{1063}$	0.983	5.377	3.926
IV* **	**F=** $\beta_0+\beta_3 p_{1009}+\beta_6 p_{511}+\beta_7 p_{626}+\beta_8 p_{1169}$	0.992	3.835	2.800
V* **	**F=** $\beta_0+\beta_3 p_{1009}+\beta_6 p_{611}+\beta_7 p_{626}+\beta_8 p_{1169}+\beta_9 p_{1591}$	0.996	2.805	2.048
VI* **	**F=** $\beta_0+\beta_3 p_{1009}+\beta_6 p_{511}+\beta_7 p_{626}+\beta_8 p_{1196}+\beta_9 p_{1591}+\beta_{10} p_{17}$	0.999	4.155	3.034
VII* **	**F=** $\beta_0+\beta_3 p_{1009}+\beta_6 p_{511}+\beta_7 p_{626}+\beta_8 p_{1169}+\beta_9 p_{1591}+\beta_{11} p_{546}+\beta_{12} p_{1242}$	0.999	1.093	0.798
VIII* **	**F=** $\beta_0+\beta_3 p_{1009}+\beta_6 p_{511}+\beta_7 p_{626}+\beta_8 p_{1169}+\beta_9 p_{1591}+\beta_{11} p_{546}+\beta_{13} p_{713}+\beta_{14} p_{1402}$	0.999	0.695	0.507

n=15; F: fracture force; β_0-β_{14}: regression coefficients; p: predictor; R^2: determination coefficient; SEP: standard error of prediction; CV: coefficient of variation; Significance: * $P < 0.05$, ** $P \leq 0.01$, *** $P \leq 0.001$.

Annex 12. Regression coefficients values for fracture force.

	Models							
	I* **	**II*** **	**III*** **	**IV*** **	**V*** **	**VI*** **	**VII*** **	**VIII*** **
β_0	67.874 ***	49.030 ***	-15.288 *	-7.519 ns	-31.092 *	- 88.733 ***	29.200 ***	37.025 **
β_1	-24.755 ***	-21.266 ***	-	-	-	-	-	-
β_2		-13479 **	-	-	-	-	-	-
β_3			1544.151 ***	1801.548 ***	1708.411 ***	1450.493 ***	1406.014 ***	1367.115 ***
β_4			40.404 ***	-	-	-	-	-
β_5			792.908 ***	-	-	-	-	-
β_6				-422.072 ***	-652.935 ***	-712.229 ***	-735.661 ***	-750.793 ***
β_7				299.418 ***	259.328 ***	290.877 ***	281.711 ***	271.441 ***
β_8				1333.231 ***	1472.614 ***	1703.917 ***	1718.469 ***	1743.167 ***
β_9					157.630 *	208.259 ***	2226.183 ***	239.346 ***
β_{10}						-0.463 **	-	-
β_{11}							7153.278 ***	8091.927 ***
β_{12}							-5.358 *	-
β_{13}								-10.805 **
β_{14}								3.460 *

n=15; β_0-β_{14}: regression coefficients; Significance: ns $P \geq 0.05$ * $P < 0.05$, ** $P \leq 0.01$, *** $P \leq 0.001$.

Annex 13. Models for the prediction of fracture distance in Frankfurters using all the optical predictors (slopes and ratios and their inverse, square and cube transformations).

Model		R^2	SEP	CV
I**	**D=** $\beta_0+\beta_1 p_{1191}$	0.438	0.735	4.958
II***	**D=** $\beta_0+\beta_2 p_{540}+\beta_3 p_{1535}$	0.793	0.464	3.131
III***	**D=** $\beta_0+\beta_3 p_{1535}+\beta_4 p_{550}+\beta_5 p_{1471}$	0.955	0.226	1.525
IV***	**D=** $\beta_0+\beta_3 p_{1535}+\beta_4 p_{550}+\beta_5 p_{1471}+\beta_6 p_{1565}$	0.966	0.207	1.398
V***	**D=** $\beta_0+\beta_3 p_{1535}+\beta_4 p_{550}+\beta_5 p_{1471}+\beta_7 p_{1115}+\beta_8 p_{1461}$	0.985	0.146	0.983
VI***	**D=** $\beta_0+\beta_3 p_{1535}+\beta_4 p_{550}+\beta_5 p_{1471}+\beta_7 p_{1115}+\beta_9 p_{1471}+\beta_{10} p_{1536}$	0.996	0.081	0.546
VII***	**D=** $\beta_0+\beta_3 p_{1535}+\beta_4 p_{550}+\beta_7 p_{1115}+\beta_{10} p_{1536}+\beta_{11} p_{335}+\beta_{12} p_{472}+\beta_{13} p_{942}$	0.999	0.029	0.199
VIII***	**D=** $\beta_0+\beta_3 p_{1535}+\beta_4 p_{550}+\beta_7 p_{1115}+\beta_{10} p_{1536}+\beta_{11} p_{335}+\beta_{13} p_{942}+\beta_{14} p_{09}+\beta_{15} p_{1149}$	1.000	0.025	0.168

n=15; D: fracture distance; β_0-β_{15}: regression coefficients; p: predictor; R^2: determination coefficient; SEP: standard error of prediction; CV: coefficient of variation; Significance: * $P < 0.05$, ** $P \leq 0.01$, *** $P \leq 0.001$.

Annex 14. Regression coefficients values for fracture distance.

	Model							
	I**	**II*****	**III*****	**IV*****	**V*****	**VI*****	**VII*****	**VIII*****
β_0	17.391***	-1.853 ns	3.975 ***	6.170 **	4.965 ***	10.456 ***	10.544 ***	7.378 ***
β_1	9.076 **	-	-	-	-	-	-	-
β_2		7886.979 ***	-	-	-	-	-	-
β_3		1131.162 ***	921.021 ***	903.459 ***	1064.459 ***	1919.947 ***	1996.105 ***	2113.562 ***
β_4			-870.433 ***	-807.972 ***	-947.071 ***	-874.688 ***	-928.092 ***	-1082.773***
β_5			6.969 ***	5.983 ***	7.561 ***	5.733 ***	-	-
β_6				-0.735 ns	-	-	-	-
β_7					60.446 **	119.670 ***	132.781 ***	133.049 ***
β_8					1.664 **	-	-	-
β_9						5.733 ***	-	-
β_{10}						-1623.332***	-1817.455***	-1998.479***
β_{11}							2.007 ***	2.033 ***
β_{12}							0.948 ***	-
β_{13}							6.600 ***	6.617 ***
β_{14}								0.008 ***
β_{15}								-0.036 ***

n=15; β_0-β_{15}: regression coefficients; Significance: ns $P \geq 0.05$ * $P < 0.05$, ** $P \leq 0.01$, *** $P \leq 0.001$.